DESIGN OF A 'SMART MANIFOLD' FOR GEOTHERMAL HVAC INSTALLATIONS

By

Michael Di Paolo

B.Eng. in Mechanical Engineering, Ryerson University, 2012

A Thesis

presented to Ryerson University

in partial fulfillment of the

requirement for the degree of

Master of Applied Science

In the program of

Mechanical & Industrial Engineering

Toronto, Ontario, Canada, 2014

AUTHOR DECLARATION

I hereby declare that I am the sole author of this thesis. This is a true copy of the thesis including any required final revisions, as accepted by my examiners.

I authorize Ryerson University to lend this thesis to other institutions or individuals for the purpose of scholarly research.

I further authorize Ryerson University to reproduce this thesis by photocopying or by other means, in total or in part, at the request of other institutions or individuals for the purpose of scholarly research.

I understand my thesis may be made electronically available to the public.

ABSTRACT

Design of a Smart Manifold for Geothermal HVAC Installations

Michael Di Paolo
Master of Applied Science
Mechanical Engineering, 2014
Ryerson University, Toronto, ON, M5B 2K3, Canada

Ground Source Heat Pump (GSHP) systems are an effective way to reduce a building's heating and cooling energy consumption. However, sizing a GSHP system to effectively meet all of a building's demand usually leads to an oversized system for the majority of any given year. Oversizing can result in an undesirable payback period. One aspect of a GSHP system's design which inhibits a reasonable payback time is the inability to effectively operate the geo-field at reduced capacity. As a result, a GSHP system will tend to run at full capacity in short bursts at a time, rather than the more efficient alternative of running for longer intervals at reduced capacity. This study introduces a design modification to GSHP systems, called a 'Smart Manifold', which enables oversized geo-fields to dynamically resize themselves, allowing for more efficient operating conditions, while still being capable of satisfying building heating and cooling.

ACKNOWLEDGEMENTS

Above all, I would like to thank my supervisor, Dr. Seth B. Dworkin, for providing me with boundless opportunities and such incredible support throughout my research. I would also like to thank my colleague at Ryerson University, Mr. Seyed Masih Alavy Ghahfarrokhy, for his expertise, time, and building energy use data. Moreover, I owe a great deal of gratitude to Groundheat Solar Wind, and its owner, Mr. Gino Di Rezze P.Eng., for sponsoring this project, and providing me with outstanding practical experience. I'd also like to thank Mr. Cid Negri P.Eng., and Salim Esmail from Groundheat Solar Wind for their vast technical knowledge. Lastly, I greatly appreciate the funding provided by NSERC, OCE, and Connect Canada.

TABLE OF CONTENTS

AUTHOR DECLARATION ii
ABSTRACT iii
ACKNOWLEDGEMENTS iv
LIST OF FIGURES vii
LIST OF TABLES ix
NOMENCLATURE x
CHAPTER 1 – Introduction 1
1.1 Motivation 1
1.2 Objectives 2
1.3 Outline 2
Chapter 2 – Literature Review 3
2.1 Overview of Current Ground-Source Heat Pump Technology 3
2.2 Open Loop Systems 4
2.3 Closed Loop Systems 5
2.4 Challenges and Advancements 7
2.4.1 Restricted Land Area 8
2.4.2 Environmental Issues and Sustainability 9
2.4.3 Thermal Energy Storage 10
2.4.4 CO_2 Heat Pipes 12
2.5 System Modeling and Balancing 14
2.6 Advantages of GSHP over Conventional Systems 14
2.7 Remarks 17
Chapter 3 – Design Methodology 18
3.1 Methodology 18
3.2 Building Description 25
3.3 Base Case, without ‘Smart Manifold’ 28
3.4 Addition of ‘Smart Manifold’ 32
Chapter 4 – Results 35
4.1 Case I – Establishing Maximum Acceptable Run Time (no ‘Smart Manifold’) 35

4.2 Case II –Minimum Flow for Turbulence (Without ‘Smart Manifold’) 38
4.3 Case III – ‘Smart Manifold’ Implementation 41
4.4 ‘Smart Manifold’ NPV, Payback Time and Emissions Saved 46
Chapter 5 – Conclusions and Future Work 50
Appendix A 52
Appendix B 54
REFERENCES 55

LIST OF FIGURES

Figure 1 – Energy Use of Average Canadian Home, (reproduced from [8]) 3
Figure 2 – Open Loop Illustration, (reproduced from [11]) 4
Figure 3 – Horizontal GSHP Loops, (reproduced from [12]) 5
Figure 4 – Vertical GSHP Loops, (reproduced from [12]) 5
Figure 5 – Pond (Surface Water) GSHP Loop, (reproduced from [12]) 6
Figure 6 – Installation of vertical boreholes, UOIT, Courtesy of Groundheat Solar Wind [4] 7
Figure 7 – Single and Double-layer Horizontal GSHP, (reproduced from [10]) 8
Figure 8 – Typical Vertical Borehole VS Improved, (reproduced from [14]) 9
Figure 9 – Ground Temperature Change and Recuperation, (reproduced from [3]) 10
Figure 10 – Monthly Heating and Cooling Demand, (reproduced from [16]) 12
Figure 11 – Heat Pipe (left) VS Conventional U-Tube (right), (reproduced from [22]) 13
Figure 12 – Heat Pump Performance Illustration, (reproduced from [26]) 15
Figure 13 – GSHP Schematic with Heating, Cooling and DHW Capability, (reproduced from [19]) 16
Figure 14 – Sample Peak Monthly Building Loads, (Data Courtesy of Groundheat Solar Wind [4]) 18
Figure 15 – Reverse-Return Borehole Branch Layout 19
Figure 16 – Typical Supply and Return Manifolds (along wall), (courtesy of [4]) 20
Figure 17 – Manifold side-view, (courtesy of [4]) 20
Figure 18 – Simplified Geo-Field Circulation Schematic 21
Figure 19 – Parallel Flow Configuration, (reproduced from [33]) 22
Figure 20 – Graphical Representation of Pump Affinity Laws, (reproduced from [35]) 23
Figure 21 – Hourly Annual Building Heating and Cooling Demand (Corrected) 26
Figure 22 – Peak Monthly Heating and Cooling Demands 27
Figure 23 – Average Daily Heating and Cooling Demands 28
Figure 24 – Effects of Fluid Temperature on Reynolds Number 29
Figure 25 – Sensitivity of Reynolds Number to Temperature at System Flow Rate of 600 USGPM 29
Figure 26 – Hourly Circulation Pump Required Supply 30
Figure 27 – Hourly Required Circulation Pump Capacity 31
Figure 28 – Yearly Frequency of Circulation Pump Load 31
Figure 29 – Corrected Yearly Frequency of Circulation Pump Load 32
Figure 30 – 'Smart Manifold' Modification 33
Figure 31 – Reynolds Number at Varying Geo-Field Size, with Fluid Temperature at 46°F 34
Figure 32 – Case I, Circulation Pump Run Time at Full Capacity 36
Figure 33 – Case I, Circulation Pump Hourly Maximum Run Time by Month 36
Figure 34 – Case I, Hourly Average Circulation Pump Run Time by Month 37
Figure 35 – Case I, Hourly Electricity Consumption 38
Figure 36 – Case II, Hourly Pump Run Time, Lowest Turbulent Flow (Without 'Smart Manifold') 39
Figure 37 – Case II, Average Hourly Circulation Pump Run Time by Month 39
Figure 38 – Case II, Hourly Pump Capacity 40
Figure 39 – Case II, Circulation Pump Electricity Consumption 40
Figure 40 – Case II, Yearly Frequency of Circulation Pump Load 41
Figure 41 – Case III, Hourly Pump Run Times 43
Figure 42 – Hourly Run Time for Cases II and III 43
Figure 43 – Case III, Difference in Minimum vs. Corrected Pump Load 44
Figure 44 – Case III, Hourly Pump Electricity Consumption 44

Figure 45 – Case III, Yearly Frequency of Circulation Pump Load 45
Figure 46 – Electricity Saved Between Case II and Case III 46
Figure 47 – Frequency of Branches Closed 46
Figure 48 – Densities of 30% Propylene Glycol, reproduced from data from [44] 54
Figure 49 – Viscosity of 30% Propylene Glycol, reproduced from data from [44] 54

LIST OF TABLES

Table 1 – Building GSHP System Details, Courtesy of [4] 26
Table 2 – Hours of the Year Belonging to Each Month 27
Table 3 – Case I Results Summary 38
Table 4 – Case II Results Summary 41
Table 5 – Case III Results Summary 45
Table 6 – Variables for NPV and Payback Calculations 48
Table 7 – Building Energy Model Results, Courtesy of [38] 52
Table 8 – Run Time and Power Consumption Results 53

NOMENCLATURE

A	Pipe cross sectional area (ft^2)
BHP	Brake Horse Power
BTU	British Thermal Unit
COP	Coefficient of Performance
CSA	Canadian Standards Association
C_p	Specific heat ($BTU/lb\,°F$)
D_h	Hydraulic diameter of the pipe (ft)
DHW	Domestic Hot Water
EER	Energy Efficiency Ratio
g	Acceleration due to gravity (ft/s^2)
GHE	Ground Heat Exchanger
GLD	Ground Loop Design
GSHP	Ground Source Heat Pump
H	Pressure head (ft)
HDPE	High Density Polyethylene
HPNC	High Performance New Construction
HVAC	Heating, Ventilation and Air Conditioning
$\dot{m}$	Mass flow rate (lb/h)
n	Pump efficiency
NPV	Net Present Value
P	Pump Power (BHP or kW)
Q	Volumetric flow rate (USGPM)
$\dot{q}$	Heat Flow Rate (BTU/h)
Re	Reynolds Number
RPM	Revolutions Per Minute
SDR	Standard Dimensioning Ratio
USGPM	U.S. Gallon Per Minute
UTES	Underground Thermal Energy Storage
VFD	Variable Frequency Drives

ΔT	Temperature difference between entering and exiting fluid ($°F$)
ρ	Fluid density (lb/ft^3)
V	Fluid velocity (ft/s)
μ	Dynamic viscosity ($lbf \cdot s/ft^2$)

CHAPTER 1 – Introduction

1.1 Motivation

Recent years have seen tremendous growth in human population, which in turn has led to a corresponding increase in energy demand. Consequently, concerns of fossil fuel depletion, environmental damage, and economic stability are becoming increasingly urgent [1]. Accordingly, worldwide efforts are being made to significantly reduce carbon emissions [2]. As a result, renewable energy sources are attracting more attention on the global scale. Geothermal energy in particular is well suited to the task of allowing the global community to move away from fossil fuels and decrease electricity consumption.

Geothermal energy is largely considered as an inexhaustible source [3]. Heat within the earth regenerates as a result of the decay of radioactive isotopes deep underneath the surface, as well as through solar radiation [3, 4]. The energy generated each year within the earth is nearly double that of global annual energy consumption [3]. The heat energy generated is normally lost to the atmosphere. However, geothermal technology utilizes this heat in a productive way before it is lost. Due to the large amount of energy produced, the high capacity for thermal energy storage, and the regenerative process, geothermal energy is considered not only as renewable, but also as sustainable for global demands as well.

When the ground is coupled with a heat pump, heating and cooling of a building can be done very efficiently. However, as with many other forms of renewable energy, long payback periods are still a great concern within the geothermal industry. The largest capital cost consideration for ground-coupled installations is the drilling of vertical boreholes. The borehole field size is primarily dependent on the soil and rock thermal properties on-site, as well as building heating and cooling demand – variables that cannot be altered for the purposes of sizing the building's heating, ventilation and air conditioning (HVAC) system. While there are efforts to develop high thermal-efficiency borehole technologies to reduce drilling, such as the Kelix Ground Heat Exchanger (GHE) [5], traditional techniques are still widespread in industrial practice. As a result, with installation practices as they presently are, reduction of payback periods is reliant on system efficiency. In the literature, as well as in practice, there still remains the capacity for efficiency improvement through intelligent management of the interface between indoor and

outdoor systems. This thesis will explore the potential for improving efficiency by introducing a variably controlled circulation pump and manifold valve system for the ground loop component of a ground source heat pump system.

1.2 Objectives

Due to the wide variation of temperatures throughout the year in much of Canada, a geothermal system that meets the entirety of a building's heating and cooling demand may be significantly oversized for much of the year. When a geothermal system is oversized, the borehole field is similarly oversized. However, unlike traditional heating or cooling systems, a geothermal system is unable to scale the capacity of the field. Either all or none of the borehole field is used. This on/off system is typical of early-stage control strategies, but is far from the ideal operation method.

The interface between the building's internal components and the geothermal borehole field is the manifold. The manifold collects all of the flows from the borehole field into a single stream. By adding control to the manifold, creating a 'Smart Manifold', the borehole field is able to be controlled and scaled as needed.

By scaling the number of boreholes in use at a given time, the circulation pumping system for outdoor components can also be scaled. It is assumed that in this operation, the heat pump is scalable and allows for variable capacity. The objectives of this project will be to analyze the effects a 'Smart Manifold' will have on an installation of a ground source heat pump system, as well as the influence on payback period, and environmental impacts.

1.3 Outline

Chapter 2 of this thesis is a literature review on geothermal energy and ground-source heat pump technologies as is related to the design of a Smart Manifold. Chapter 3 is an in-depth explanation of the objectives as well as the methodologies used in evaluating the Smart Manifold design. Results and applications of implementing the novel manifold design will be discussed in Chapter 4. The thesis ends with concluding remarks and future study paths, included in Chapter 5. Despite the norm of using SI units in Canada at the time of this publication, imperial units are used herein to conform to industry practices.

Chapter 2 – Literature Review

2.1 Overview of Current Ground-Source Heat Pump Technology

Geothermal energy comes in two primary forms. The first is high-grade geothermal energy, which typically is used today for power generation. The second, and the focus of this review, is low-grade. Low-grade geothermal energy is typically used for space heating, water heating, and cooling, but also for a variety of applications such as crop drying and snow melting [6]. This energy can be used directly to condition a space; however, not all low-grade geothermal sources are suitable for direct application. In the cases where direct application is unsuitable, a ground-source heat pump (GSHP) is employed to provide heating, cooling, or both [4].

In the majority of buildings worldwide, heating and cooling accounts for at least 40% of the total energy consumption [7]. By contrast, Canadian homes use 65% of their total energy for space heating and cooling, with an additional 20% used for heating water, as given by Natural Resources Canada and shown in Figure 1 [8]. By implementing a GSHP, energy no longer has to come from the combustion of fossil fuels to provide heating. Because of the extremely high efficiencies of GSHPs, electrical demand can be reduced in cooling mode when compared to conventional air conditioning systems. This chapter investigates the different types of GSHP systems currently available and their applications, and evaluates their advantages, challenges, and advancements.

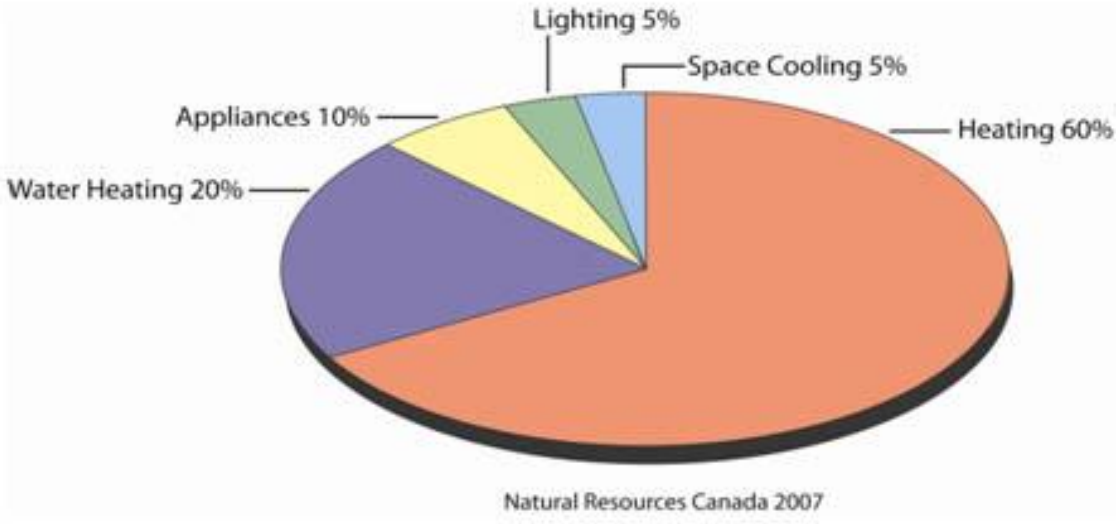

Figure 1 – Energy Use of Average Canadian Home, (reproduced from [8])

In the simplest terms, a heat pump is a device that uses electrical and mechanical energy to move heat energy against a temperature gradient via a compression and expansion cycle [4]. The earth has an approximately constant seasonal temperature under 5 meters [9], and its size and thermal properties make it an ideal medium to allow a heat pump to meet building requirements and operate efficiently. Earth, groundwater, and surface bodies of water can all be used as heat sources and storage media from which heat can be extracted, and into which heat can be dumped [10]. Coupled with the earth, the heat pump can extract heat from the ground and dump it into a dwelling, or the process can be reversed, extracting heat from the dwelling and rejecting it into the ground. As such, one heat pump can provide both the heating and cooling required. Extracting or rejecting can be accomplished by a fluid moving through the system in either an open or closed-loop set-up.

2.2 Open Loop Systems

In an open system, the heat transfer fluid is water pumped out from underground resources like aquifers [11]. This water can sometimes be used directly for cooling, if the temperatures are cold enough, or passed through a heat pump to generate the temperatures required. Once the heat has been transferred into the building, it is then re-injected into the well to recover the heat loss or gain, and the cycle continues. This process is illustrated in Figure 2. Open loop systems need to meet stringent environmental regulations, as they can change groundwater chemistry and biology, severely reducing groundwater quality [2].

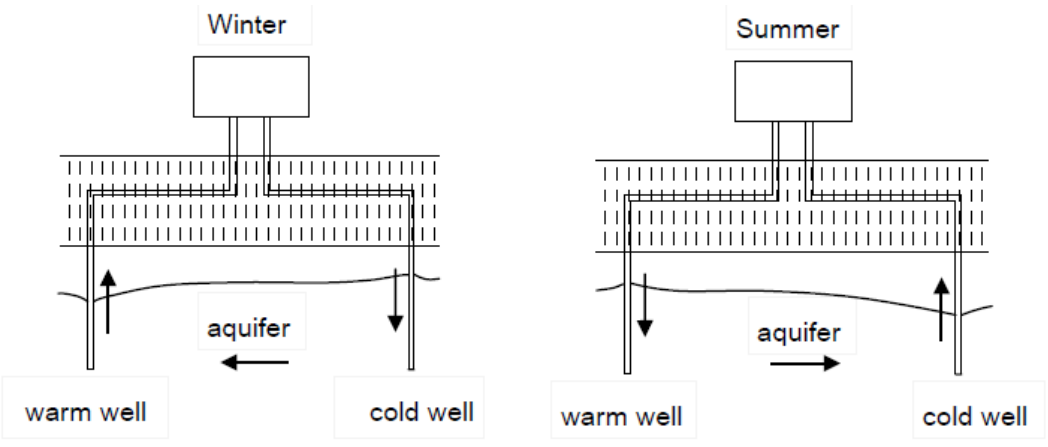

Figure 2 – Open Loop Illustration, (reproduced from [11])

2.3 Closed Loop Systems

A closed loop system differs from an open loop in that the working fluid never leaves the piping infrastructure [4]. Closed systems tend to be more expensive and less efficient than open systems, but can be installed in more locations and do not pose as significant risks to groundwater via contamination [11]. These systems consist of long lengths of pipe buried in the ground in either horizontal or vertical configurations, through which a fluid is passed to absorb or reject heat energy. The McQuay Geothermal Heat Pump Design Manual [12] illustrates three common closed-loop systems, as seen in Figures 3, 4, and 5, which are horizontal loops, vertical loops, and pond loops, respectively.

Figure 3 – Horizontal GSHP Loops, (reproduced from [12])

Figure 4 – Vertical GSHP Loops, (reproduced from [12])

Figure 5 – Pond (Surface Water) GSHP Loop, (reproduced from [12])

Currently, the most commonly used material for piping is high density polyethylene (HDPE), due to its high flexibility, durability, and longevity. HDPE is lightweight, easy to work with, and much less costly than materials with higher thermal conductivity like copper [4]. HDPE pipes are delivered in coils, and pipe fittings are fused in the field at the installation site. In horizontal installations, pipes can be coiled in their trenches to increase pipe length, which correlates to heating and cooling capacity, or simply laid out as in Figure 3, then backfilled with the excavated earth from trench digging. Vertical installations most often are installed in a simple U-bend configuration, as in Figure 4, drilling 5-inch diameter boreholes usually between 200 – 650 feet, and sometimes deeper [4]. Installed loops routinely undergo pressure testing to ensure quality and that there are no leaks [4].

Usually, the system moves water through the ground loops, but in colder climates where the ground freezes during the winter, a water-antifreeze solution is used instead [12]. However, introducing antifreeze into the system often reduces heat transfer capability, increases pump work required, and raises concerns of groundwater contamination in the event of a leak. As such, due to groundwater protection laws in certain areas, some antifreezes are banned, no matter how leak-proof a ground-loop is [2]. In Ontario, Canada, one of the more commonly used antifreezes approved by the Ministry of the Environment and CSA Standards is propylene glycol, usually in a 20-30% concentration mixture with water [4].

In the case of most vertical borehole installations, after the drilling is complete and the U-bend pipe inserted, grout or backfill comes next to fill the air spaces between the pipe and the borehole walls. In some cases where the borehole is entirely encased in rock, water can be used in place of grout [13]. Since air is an insulator, it can severely affect a borehole's performance, so displacing the air is vital. Figure 6 shows a nearly completed vertical installation in Ontario, Canada. The yellow caps are where the vertical boreholes are drilled.

Figure 6 – Installation of vertical boreholes, UOIT, Courtesy of Groundheat Solar Wind [4]

2.4 Challenges and Advancements

There are many challenges facing GSHP system designers. Challenges in design can result in poor performance with economically infeasible payback periods, as well as damage to the environment. There are also physical restrictions and limitations of GSHP applications that discourage the industry's growth. While there are significant challenges, many important advancements have also been made.

2.4.1 Restricted Land Area

One of the primary challenges faced by GSHP designers is how much land area they have to work with. Appropriate lengths of piping are installed to meet heating, cooling and hot water demands of a specific site, as determined by building energy models. Since drilling vertical boreholes is a major cost of the overall system, it is usually avoided whenever possible, and trenching for horizontal loops − a much cheaper option − is chosen instead. Vertical installations can be twice as expensive per ton of heating or cooling capacity, as compared with horizontal ones, but horizontal installations require approximately ten times the land area [4, 12]. As a result, in Canada, horizontal systems are typically reserved for low-demand residential applications with large plots of land.

In their 2009 study, Tarnawski *et al.* [10] investigate the relationship between depth of horizontal installations and coefficient of performance (COP). They established that increasing a horizontal loop's depth under the surface had a positive effect on both heating and cooling efficiencies. However, despite the increased COP from the deeper loops, the recommendation was to still use a shallower trench for the horizontal installation, due to efficiency gains being overshadowed by the cost of additional excavation [10]. The study also showed that a stacked configuration of horizontal loops is feasible and effective if land area is restricted, as shown in Figure 7. The stacking of loops can reduce the required land area by about half [10].

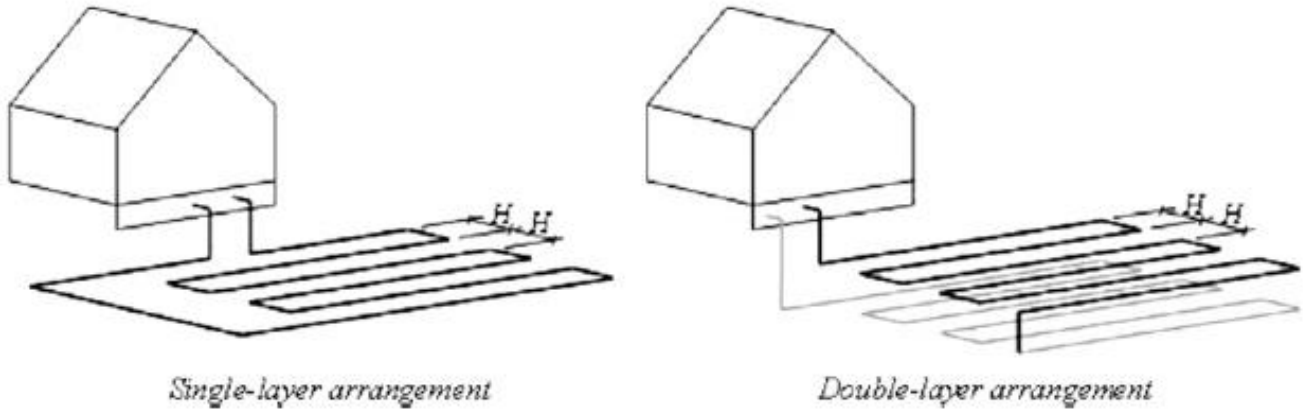

Figure 7 – Single and Double-layer Horizontal GSHP, (reproduced from [10])

Another method of saving space and money is to reduce the number of vertical boreholes drilled. If fewer boreholes are drilled, initial capital cost is reduced, but the capacity of the field to

supply building loads suffers. Increasing each borehole's ability to transfer heat can reduce the overall number of holes required. One method, shown in Figure 8, is to increase the ratio of pipe surface area to that of the borehole wall, and at the same time decrease the temperature interference between supply and return lines [14]. The result is a 30-50% reduction in borehole length, and an overall cost saving of almost one third, based on test holes and Ground Loop Design (GLD) models [14].

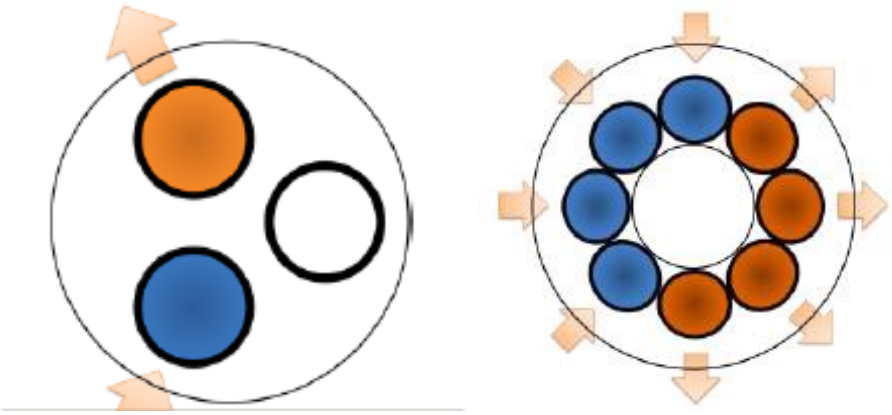

Figure 8 – Typical Vertical Borehole VS Improved, (reproduced from [14])

2.4.2 Environmental Issues and Sustainability

To be truly sustainable, a GSHP can neither deplete the thermal resources of the source, nor can it be detrimental to the environment. Source depletion and environmental damage often go hand-in-hand, as there can be significant chemical and biological impacts, especially on groundwater in open loop systems [2]. Most GSHP vertical systems, even with unbalanced heat extraction or rejection, can achieve thermal equilibrium. In the first few years of heat extraction, there is a rapid change in ground temperature. This cooling creates a temperature gradient that draws more heat into the vertical boreholes, effectively creating a new thermal equilibrium [3, 15]. Figure 9 illustrates the rapid change in ground temperature in the first several years, followed by a much more gradual change as the temperature gradient in the ground adapts. The recuperation in Figure 9 shows how the ground temperature recovers once the GSHP system has been shut off. Again, it can be seen that there is a large change in ground temperature in the beginning, until a new equilibrium becomes established.

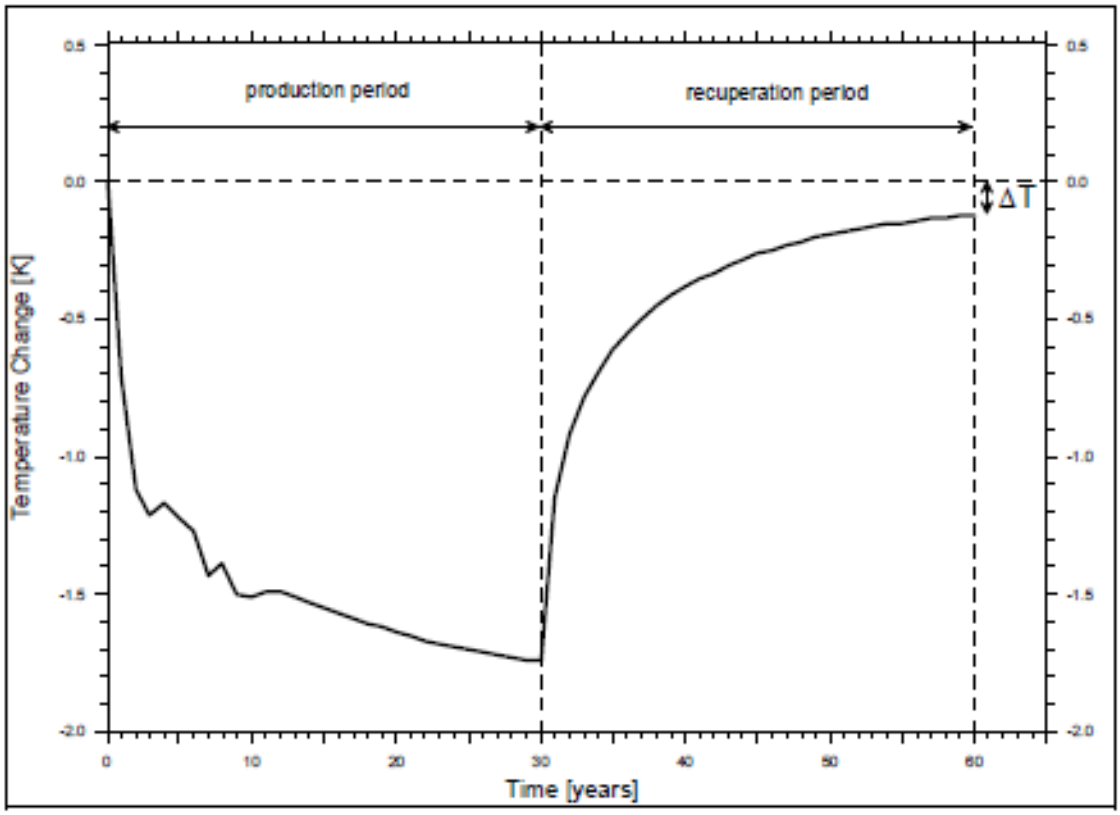

Figure 9 – Ground Temperature Change and Recuperation, (reproduced from [3])

2.4.3 Thermal Energy Storage

In Canada, and elsewhere in the world, buildings require both heating and cooling. Heat is extracted from the ground in the winter, and in the summer, heat is rejected to the ground. This is a basic form of seasonal Underground Thermal Energy Storage (UTES) [4]. By balancing the system's heating and cooling requirements over the course of a year, the GSHP has less of an impact on natural ground temperature equilibrium. A change in ground temperature also adversely affects heat pump efficiency over time, since the designed loop temperature will change year after year [12].

Even in cold climates, large commercial buildings often demand more cooling than heating capacity [4]. As a result, the GSHP rejects more heat into the ground than it extracts. The resulting increase in ground temperature lessens system efficiency, and creates a finite lifetime for the system if the imbalance is greater than what can be overcome by the ground's recharge rate. UTES paired with complementary technologies to GSHPs can make good use of the load imbalance.

One such technology is a desuperheater, which increases the heat production of the GSHP in order to provide domestic hot water (DHW) [4]. Recalling Figure 1, Canadian homes use approximately 20% of their total energy for water heating. Since cooling dominant buildings will reject more heat than they use, a desuperheater merely takes advantage of the waste heat to create DHW, increasing the system's overall usefulness and cost effectiveness. Unfortunately, desuperheaters are somewhat limited as they cannot generate sufficiently high temperatures to kill legionella bacteria, so a supplementary boosting system may be required [4].

However, not all loads can be balanced by long term seasonal recharging. Fernandez *et al.* [16] provides an example where the cooling load dominates to such a large degree that the seasonal re-cooling during winter comes nowhere close to balancing the system. As shown in Figure 10, the seasonal heat extraction is unable to re-cool the ground sufficiently to meet yearly cooling demand. In a conventionally balanced GSHP system, all of the heating requirements would be satisfied, but only about 7% of cooling would be met [16]. However, the investigators noted that UTES can also be utilized on a short-term basis. This means that air temperatures on summer nights were sufficiently low to re-cool the GSHP. In this way, an increase to 13% from 7% of total cooling load was satisfied [16]. Similar results of the effectiveness of short term TES were shown by Abbas and Sanner [17] in Egypt, where ground temperature is also high and cooling demand dominates. It is unclear from the report whether Fernandez *et al.* used a desuperheater to provide hot water, which would further increase heat extraction and thus enhance re-cooling. However, due to such high yearly ambient temperatures, it is likely that a solar water heater was implemented instead.

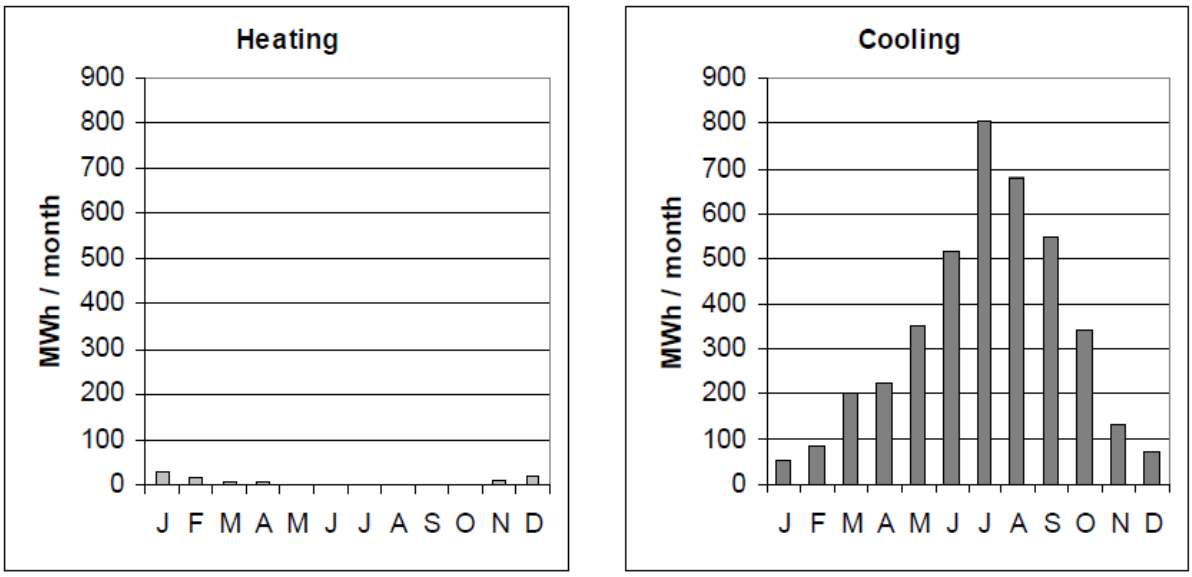

Figure 10 – Monthly Heating and Cooling Demand, (reproduced from [16])

There are many complementary technologies that can be applied to GSHP systems to increase efficiency and ensure optimal performance. However, the ways in which these technologies are utilized can impact their contribution. Kjellson *et al.* [18] examined which way a solar-thermal collector should be used in conjunction with a GSHP. The study found that the most beneficial way to use solar-thermal heat depended on system design, borehole depth, and seasonal variations in temperature. The heat from solar-thermal generation could be used to recharge the GSHP, or to produce DHW. It was found that electricity savings were greatest when solar-thermal was used for DHW production in the summer, and then switched to a UTES re-heating in the winter [18]. In other studies, solar heat collection and injection to recharge the ground was more advantageous due to COP gains [19]. Moreover, as ground temperature rises, heat losses to the environment increase drastically, negating the benefits of UTES [20]. These examples demonstrate that without proper design and control systems that are able to react to individual scenarios, a complementary technology like solar-thermal may not have a significant contribution. Dynamic controls are needed.

2.4.4 CO_2 Heat Pipes

Rather than use a water-antifreeze mixture in a HDPE vertical ground loop, it has been suggested that a heat pipe could be used for a variety of improved conditions. In some locations,

glycol and other antifreezes are forbidden as a result of concerns for groundwater contamination; conventional systems would not be allowed to be installed in such areas. In contrast, a heat pipe uses two-phase carbon dioxide, which has no groundwater contamination potential [21]. A heat pipe utilizes the thermosyphon effect, which is essentially a passive method that drives the evaporation and condensation of carbon dioxide. Figure 11 shows a comparison between how the flow in a heat pipe looks in comparison to a conventional U-bend vertical borehole. In a heat pipe, the heat in the ground at the bottom of the pipe causes evaporation of the refrigerant. As the refrigerant vapor rises and reaches the top, it encounters a heat exchanger and condenses, transferring its latent heat [22]. It should be noted that this self-driven system does not require a circulation pump like a conventional system would, and thus saves energy. Moreover, heat pipe GSHP systems boast an 11% and 25% COP increase, in heating and cooling modes respectively, over conventional systems [21]. The limiting factor with heat pipes is the high material costs. The pipe itself is made of flexible corrugated steel, and the heat exchanger is intricate and expensive to manufacture [21]. At the moment, it is unclear whether the COP increase is worth the capital cost increase, as GSHP systems are criticized for being expensive even with conventional installation methods and materials. More calculations for benefit-to-cost ratios would be needed.

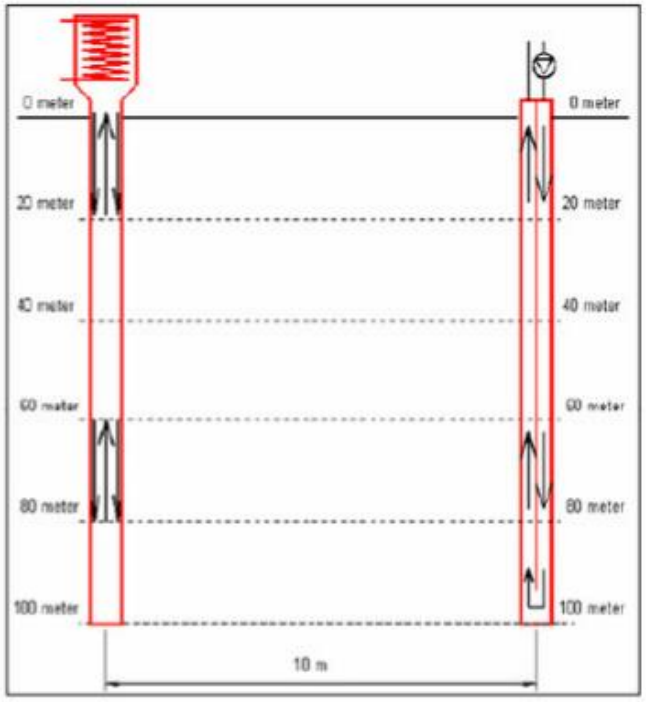

Figure 11 – Heat Pipe (left) VS Conventional U-Tube (right), (reproduced from [22])

2.5 System Modeling and Balancing

System modeling is an incredibly important step in the design process. Small projects can sometimes be handled by rules of thumb and experience designing similar systems in the region [4]. By completing an energy model of a residential, commercial or industrial building, it becomes apparent whether the heating and cooling demands are balanced, or if there is one clear dominating mode. Two common energy modeling software packages in North America are eQUEST [23] and TRNSYS [24]. After energy modeling, the monthly or hourly heating and cooling loads are known. Kjellsson *et al.* note that economically designed systems in cooler climates cover between 50-70% of the maximum peak heating load and 85-95% of the total annual heating demand [18]. Simulation tools using tools like GLD (Ground Loop Design) [25] may recommend designs that cover more or less than Kjellsson *et al.* suggest.

GLD is a software package that uses inputs from thermal response tests, design parameters like grout conductivity, and peak loads to give the required horizontal or vertical loop length. Thermal response testing measures the geothermal characteristics of a test borehole, and is considered one of the most important steps in system design. RETScreen is simpler than GLD, and provides basic payback and carbon emission reduction calculations [4]. Unfortunately, neither of these tools is sufficient to design a fully balanced, sustainable GSHP system. As such, designing a fool-proof system remains a challenge until more comprehensive tools become available.

Overall, GSHP systems are difficult to optimize. A designer may choose a larger field to reduce temperature fluctuations in the ground, but by doing so, optimal heating or cooling temperatures may not be reached. Heating is more efficient when loop temperatures are higher, but if a field is oversized to prevent potential depletion, the field may not be charged with enough heat by the end of the summer, and *vice versa* [7]. Also, oversizing a field may be very beneficial in terms of storing heat, if that application presents the most opportunities. The trade-offs in modeling are numerous in terms of performance, cost and energy consumption, so the only way to ensure the best design is to explore the entire space of all combinations. However, such a time-consuming exercise is not normally feasible in industrial applications.

2.6 Advantages of GSHP over Conventional Systems

Heat pumps boast excellent efficiencies, as illustrated by Figure 12, given by the Fundamentals of Commercial Geothermal Wellfield Design Handbook [26]. In terms of industry

terminology, efficiency in heating mode is referred to as COP, and efficiency in cooling mode is commonly referred to as the energy efficiency ratio, EER. Cooling is sometimes also given a COP rating, as opposed to EER. COP in heating mode is defined by Equation 1 as,

$$COP_H = \frac{Energy\ Gained\ (Thermal)}{Energy\ Input\ (Electrical)} \quad (1)$$

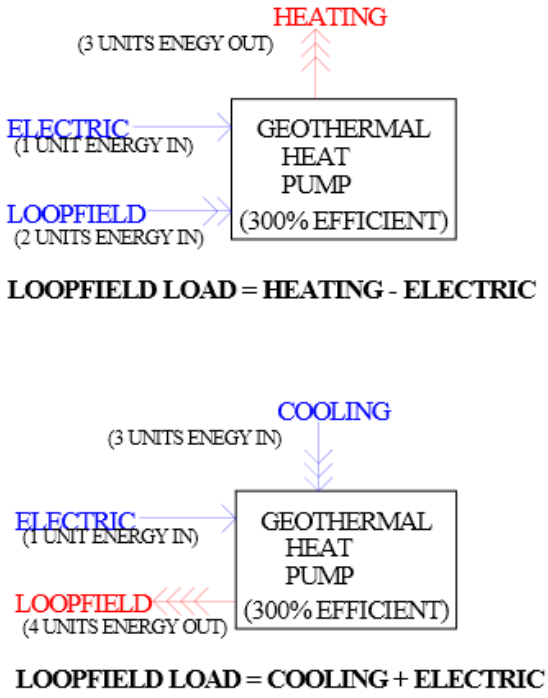

Figure 12 – Heat Pump Performance Illustration, (reproduced from [26])

So, in Figure 12, the COP of the system would be 3, correlating to 300% efficiency. The combined COP of heat pumps can see values ranging from around 3 - 5 [1, 4, 12], since they can take advantage of the stored energy in the earth. Heat pumps move heat energy, rather than create it, which is how such high COPs are attained. In contrast, typical modern fossil fuel burning furnaces have efficiencies ranging from approximately 85 - 95%, or a COP of 0.85 - 0.95 [27]. Figure 13 shows an example of a typical GSHP schematic, where the system is able to provide heating, cooling, and hot water.

A heat pump in cooling mode also sees significant efficiency gains over traditional air conditioning units, or cooling tower systems. The McQuay Geothermal Heat Pump Design Manual attributes this increase to the fact that GSHPs typically operate at a lower design temperature:

when the loop temperature is colder, the heat pump provides cooling more effectively. However, conventional systems have higher operating temperatures, and therefore produce lower energy efficiency ratios. Due to smaller natural temperature fluctuations in the ground than those of the ambient air, cooling can be provided more efficiently by GSHPs than by conventional means [19].

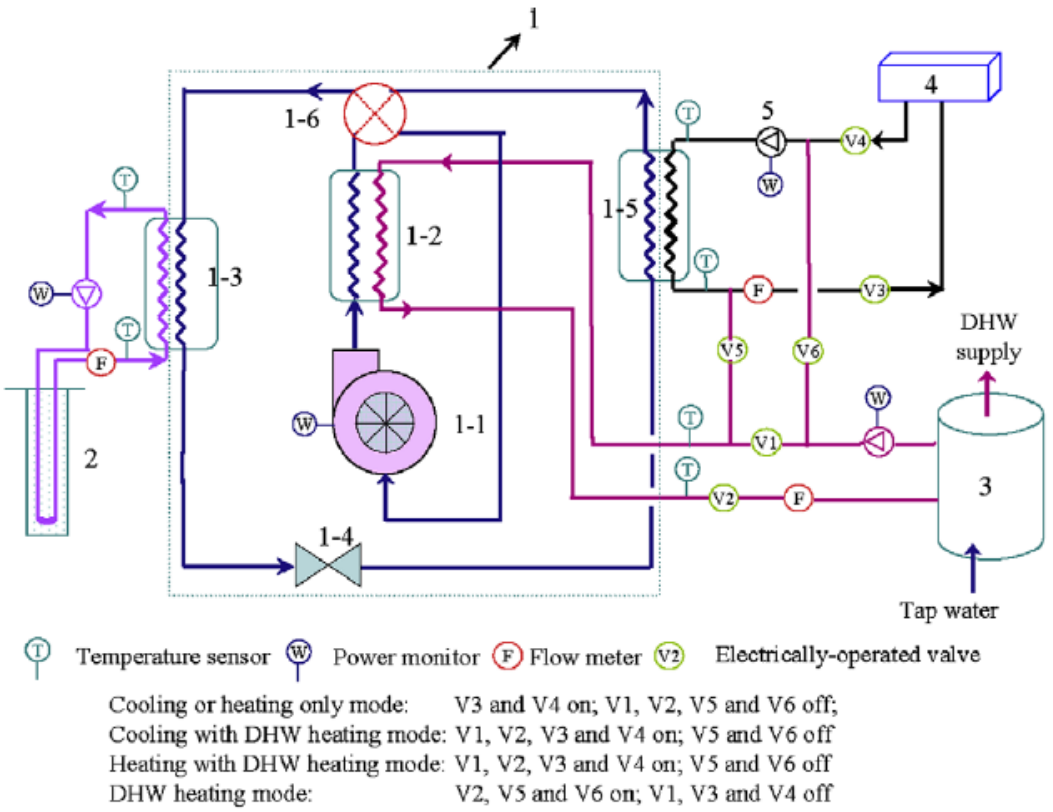

1: water-to-water heat pump; 2: GHE; 3: thermal storage tank; 4: FCU; 5: water pump

For heat pump, 1-1: compressor; 1-2: desuperheater; 1-3: condenser; 1-4: expansion valve; 1-5: evaporator; 1-6: reversing valve

Figure 13 – GSHP Schematic with Heating, Cooling and DHW Capability, (reproduced from [19])

There are numerous ways that a GSHP can be configured, and even similar configurations can differ with location, local weather, and the like. As such, it is not within the scope of this review to compute payback times on a case-by-case basis. That notwithstanding, the literature reviewed suggests a very reasonable payback period. According to Di Rezze and Negri of Groundheat Solar Wind [4], simple payback due to energy costs compared to conventional systems typically occurs within 7-9 years for GSHP systems in Ontario, Canada for commercial or large residential installations. Similarly, Desmedt *et al.* predict an 8 year simple payback period for an

office building in Belgium utilizing a vertical GSHP system [28]. Dincer and Rosen's study indicate the energy monitoring logs at the University of Ontario Institute of Technology's GSHP system suggest a 7.5 year simple payback [29]. Still, others like Midttomme *et al.* predict a longer simple payback period of 12 years [30].

After the payback period, the GSHP system becomes a return on investment. Furthermore, a global effort is being made to provide incentives to reduce energy use. An excellent opportunity in Ontario, known as High Performance New Construction (HPNC), offers building owners up to $800 per kW of energy saved [31], which can substantially reduce GSHP system capital costs, especially for large projects with big capacities [4].

In addition to attractive payback periods, GSHP systems offer many other benefits that often get overlooked. Not only does a GSHP system save energy, it also saves money on system maintenance [27], which can be a significant cost in conventional systems [32]. Additionally, Di Rezze and Negri of Groundheat [4] noted that GSHP mechanical rooms are a fraction of the size of conventional ones, and also potentially eliminate the need for large chillers on rooftops. This reduced space requirement consequently increases leasable space, a consideration that is not usually included in payback calculations. Furthermore, in areas with a high proportion of renewable electricity, GSHP systems can produce up to 77% less carbon emissions [1], and generate income through carbon credits [4].

2.7 Remarks

Geothermal usage has been around for centuries in direct applications like hot springs, and even GSHP applications are not new. A solid understanding about how the systems operate and what constitutes a good system already exists. However, there is still significant room for improvement with modeling software to produce a truly optimal design that is sustainable, cost effective, and environmentally friendly.

Chapter 3 – Design Methodology

3.1 Methodology

A GSHP system includes components inside the building operating in conjunction with a network of subterranean piping. The entire system is sized for the peak demand and extreme weather, and so it is oversized for the rest of the time. Some components inside the building, such as centrifugal pumps, have the ability to increase or decrease its capacity as required, using Variable Frequency Drives (VFDs), allowing for energy savings when running below design capacity. Modern heat pumps also allow for variable capacity, allowing for longer run times at reduced capacities. However, the underground system of piping, sometimes referred to as a geo-field, lacks the same potential to scale in combination with the rest of the system. The result is that the geo-field can be oversized for a large portion of the year. Since the GSHP system operates as a whole, not being able to scale the geo-field restricts the ability to save energy from scaling other components. Figure 14, created from energy model information provided by Groundheat Solar Wind, is an example of a system that is cooling dominant with the majority of building demands well below the peak value.

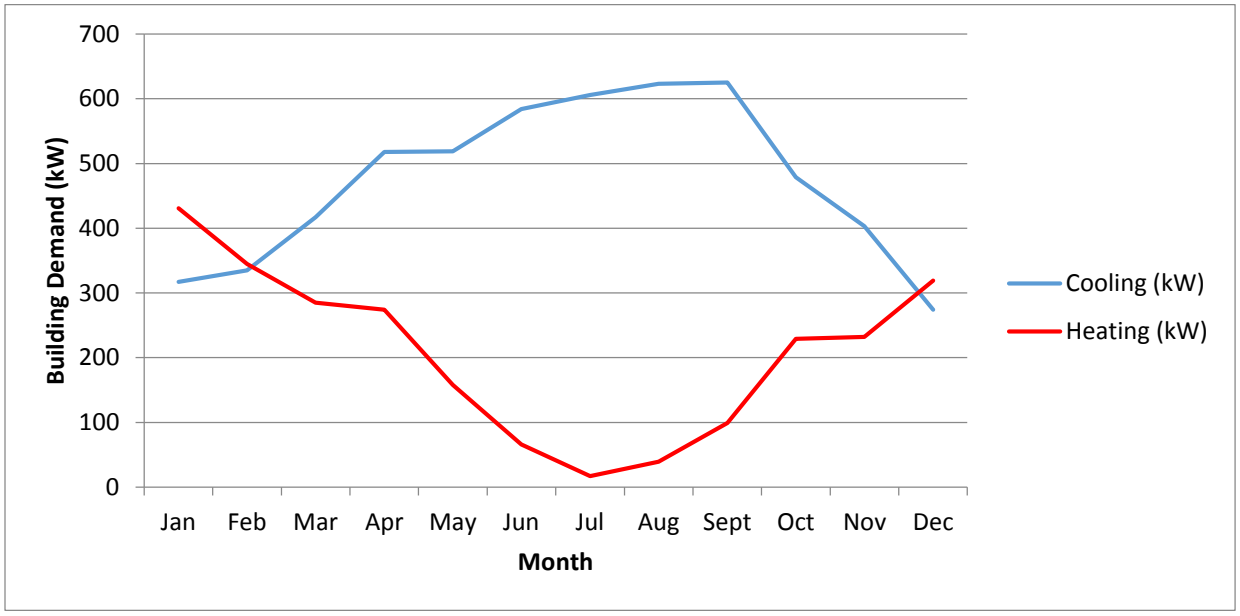

Figure 14 – Sample Peak Monthly Building Loads, (Data Courtesy of Groundheat Solar Wind [4])

In a vertical borehole GSHP system, boreholes are grouped into branches and connected in a reverse-return style as illustrated by the schematic in Figure 15. Boreholes are connected in reverse-return fashion to help equally distribute flow and pressure across all lines. Moreover, grouping boreholes in branches saves space in the mechanical room. Manifolds can be very large, as seen in Figures 16 and 17, so grouping boreholes in branches is an important space-saving technique for mechanical room designs.

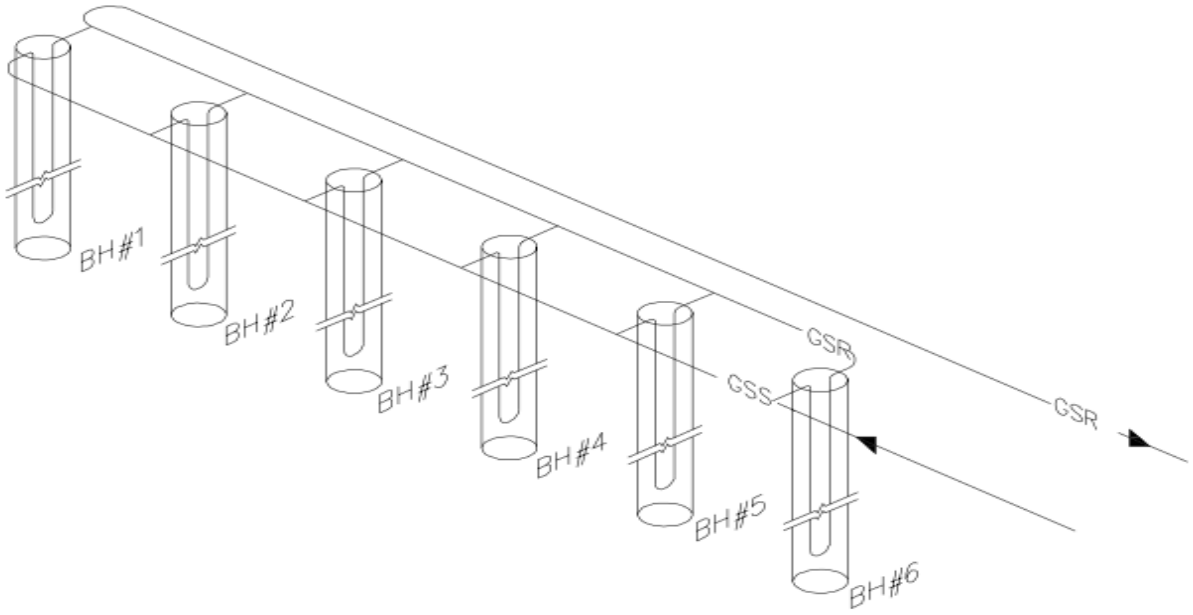

Figure 15 – Reverse-Return Borehole Branch Layout

Large systems typically have several branches, with each branch containing an equal number of boreholes. The branches interface with the building via two manifolds, one which combines all supply flows, and the other combines all return flows. A simplified schematic of a manifold circulation system within a mechanical room can be seen in Figure 18. Examining the schematic in Figure 18, the process follows a fairly linear process. Heat transfer fluid, typically a solution of propylene glycol, flows from the geo-field branches, which is then collected in the supply manifold and streamlined into a main supply line. The collected flow then passes through a heat exchanger, exchanging heat with the building's main heat-pump water loop, and then returns back to the geo-field return manifold where the flow is distributed to each branch.

Figure 16 – Typical Supply and Return Manifolds (along wall), (courtesy of [4])

Figure 17 – Manifold side-view, (courtesy of [4])

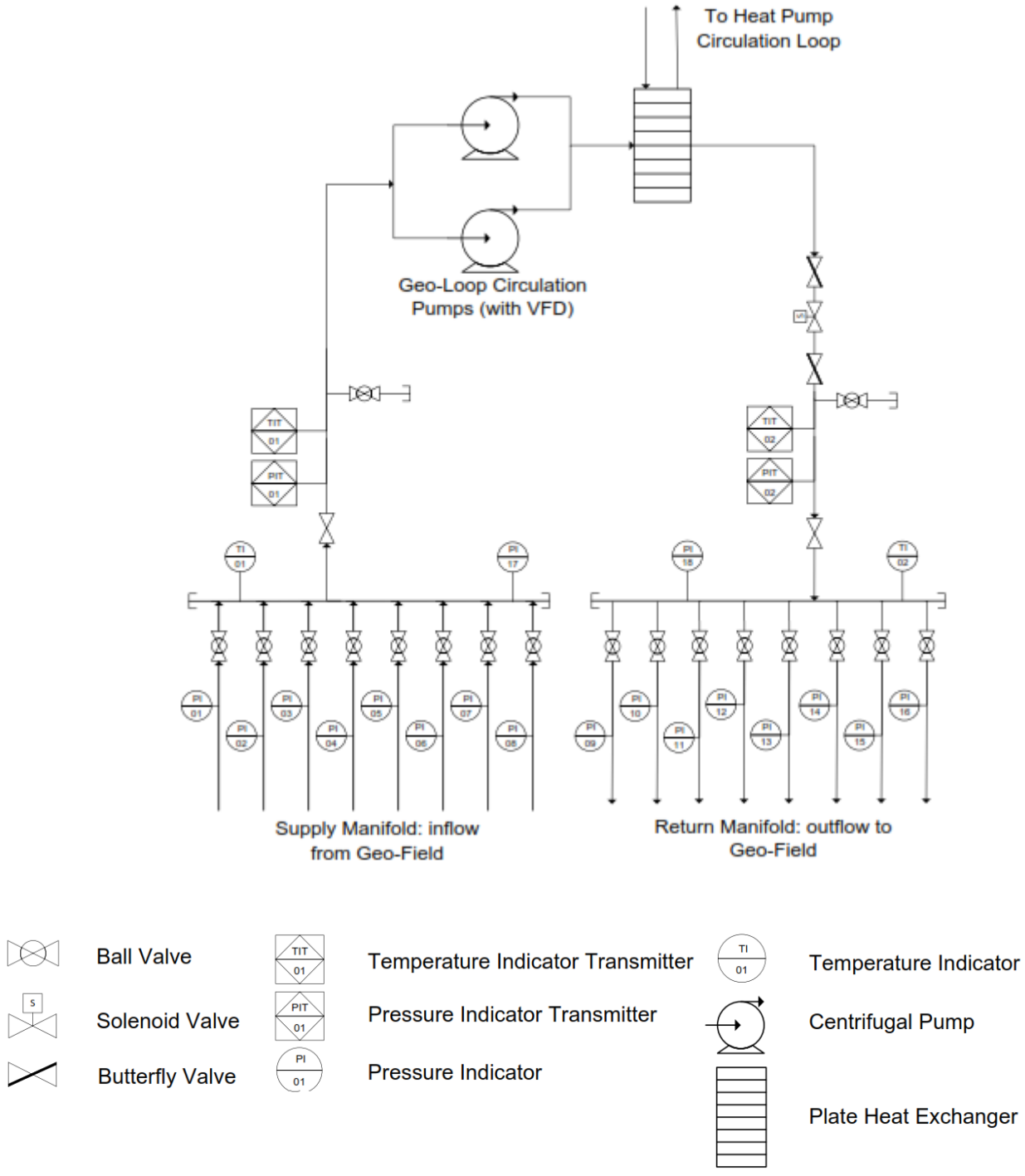

Figure 18 – Simplified Geo-Field Circulation Schematic

The branches each connect to the manifold independently, which results in a parallel flow pattern. Parallel flow is illustrated in a simplified form in Figure 19. The result is that the total flow is equalized over each branch. Parallel flow can be expressed as:

$$Q_{Total} = Q_1 + Q_2 + \cdots + Q_n \quad (2)$$

Where:

Q_{Total} = Total system volumetric flow rate (USGPM)

Q_i = Volumetric flow rate in branch *i* (USGPM)

The unexploited advantage of the parallel configuration in a GSHP system is that isolating and closing off any of the branches causes the flow rate in the remaining branches to increase without having to also increase the total system flow rate.

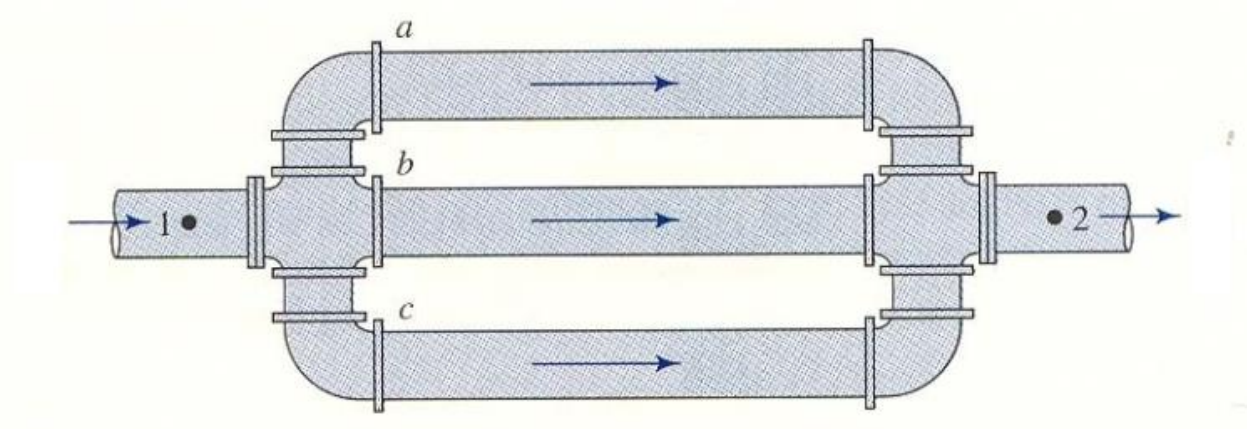

Figure 19 – Parallel Flow Configuration, (reproduced from [33])

The flow through the geo-field is driven by centrifugal pumps located in the mechanical room of the building. The geo-field circulation pumps are connected in parallel for redundancy. At any given time, only one pump is active, and the yearly loading is balanced between the two. Centrifugal pumps are capable of adjusting their motor speed and torque, by way of a variable frequency drive (VFD), to produce a different flow rate as required. The advantage of scaling the pump's output is given in Equations 3 and 4 shown in Figure 20 [34, 35]:

$$\frac{Speed_1}{Speed_2} = \frac{Flow_1}{Flow_2} \quad (3)$$

$$\frac{Power_1}{Power_2} = \left(\frac{Flow_1}{Flow_2}\right)^3 \quad (4)$$

$Speed$ = the pump speed (RPM)

$Flow$ = the pump output flow rate (USGPM)

$Power$ = the pump power required (kW)

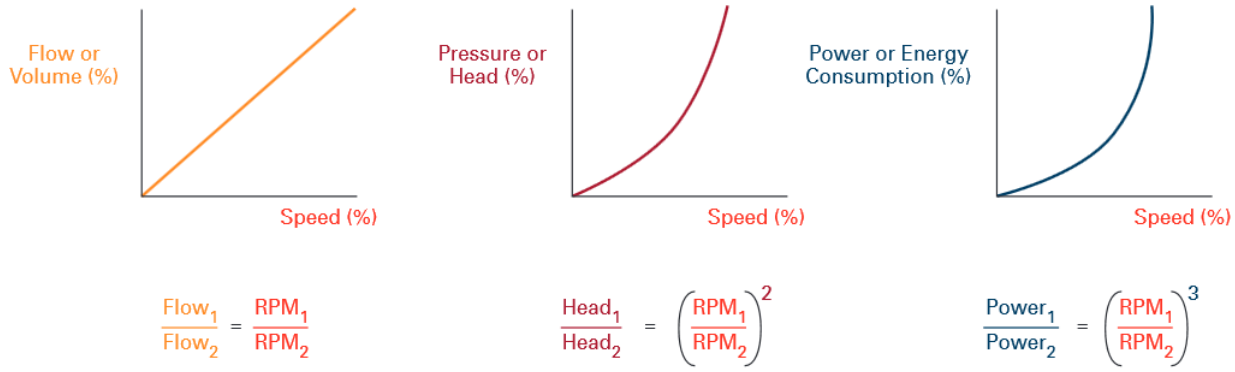

Figure 20 – Graphical Representation of Pump Affinity Laws, (reproduced from [35])

In essence, reducing flow rate when it is not needed reduces the power consumption of the pump drastically. VFDs alter the operating frequency of a pump, which allows for changing of pump speed as well as torque. Equation 4, which shows pump power savings as flow is reduced, comes from applying conservation of energy laws to the Navier-Stokes equations for momentum of a fluid. Not only do VFDs allow for significant energy savings, they also allow for soft-start, or a gradual ramp-up of pump speed, helping to preserve the life of the equipment [36]. Since GSHP systems have the potential to be oversized, recalling Figure 14, and so VFDs are typically installed in geo-field circulation pumps. However, changing the rate at which fluid flows through the geo-field changes important properties that affect system performance.

The first property that changes as a result of a change in fluid flow rate is the rate of heat transfer. A GSHP system requires heat to be extracted from, or rejected into, the ground through the geo-field. The rate at which heat transfer occurs is given by Equation 5 [37]:

$$\dot{q} = \dot{m} C_p \Delta T \tag{5}$$

Where:

$\dot{q}$ = heat transfer rate (BTU/h)

$\dot{m}$ = mass flow rate (lb/h)

C_p= specific heat capacity ($BTU/lb\,°F$)

ΔT = temperature difference between entering and exiting fluid ($°F$)

If it is assumed that the specific heat capacity and temperature difference each remain constant, then heat transfer rate is directly impacted by the mass flow rate. In this case, lowering volumetric flow rate, and thus mass flow rate, will result in a proportionately lower heat transfer rate. Mass flow rate is related to volumetric flow rate by:

$$\dot{m} = Q \times \rho \tag{6}$$

ρ = fluid density (lb/ft^3)

The second property that is affected as a result of changing volumetric flow rate is the Reynolds number (Re). In fluid flow applications, the Reynolds number is used to predict whether flow is laminar or turbulent [34, 37]. GSHP systems are typically designed to maintain high Reynolds number values, which correspond to turbulent flow, and an associated increase in convective heat transfer. Turbulence increases the mixing of the flowing fluid, thereby rapidly redistributing energy throughout the fluid and increasing convective heat transfer. Heat transfer is highest at turbulent flow [37]. By contrast, in laminar flow, a thermal boundary layer forms along the pipe wall, inhibiting heat transfer. GSHP system designers endeavor to maintain turbulent flow, which is satisfied when $Re > 4000$ [37]. Reynolds number is a dimensionless property given by Cengel and Ghajar [37] for pipe flow as:

$$Re = \frac{\rho V D_H}{\mu} \tag{7}$$

Re = Reynolds number

V = velocity of the fluid (ft/s)

D_H = hydraulic diameter of the pipe ($inch$)

μ = dynamic viscosity ($lbf \cdot s/ft^2$)

and:

$$V = \frac{Q}{A} \tag{8}$$

A = cross sectional area of the pipe (ft^2)

When a building's heating or cooling demand drops, the amount of heat extraction or rejection from or into the ground also decreases. Recalling Equation 5, the rate at which heat is transferred to or from the ground can be altered by the flow rate. So, by lowering flow rate, circulation pump energy can be saved when heat transfer demands are low. However, lowering flow rates can transition flow from turbulent to laminar, negatively impacting heat transfer efficiency in the boreholes. An optimal solution must therefore maintain turbulence while allowing for energy savings from pump speed reduction. The 'Smart Manifold' allows for such a solution. By isolating and deactivating geo-field branches that are not required, the reduced total system flow rate is divided into fewer boreholes, which keeps flow per active borehole high, and maintains turbulence. In addition, the 'Smart Manifold' requires a variable capacity heat pump in order for dynamic changing of heat extraction or rejection.

In a typical installation, the geo-field circulation loop is outfitted with numerous instruments to measure pressure and temperature at various locations. The instruments are vital to system start-up, as well as maintenance. A 'Smart Manifold' takes advantage of this configuration by controlling which branches are active from the supply manifold.

3.2 Building Description

The building used for the case study in this thesis is a high-rise residential unit located in Toronto, Ontario, Canada. The heating and cooling for the building is supplied by a vertical borehole GSHP system. A summary of building-specific GSHP system information, provided by Groundheat Solar Wind, is summarized in Table 1. The hourly energy model for the building can be seen in Figure 21, created from an eQUEST building simulation [38]. Results of the energy model are given by hour of the year, for a total of 8760 data points. Table 2 shows which hours fall under each month. The energy model initially allows for both heating and cooling to be supplied simultaneously during each hour interval, however for the corrected heating or cooling shown in Figure 21, only either heating or cooling can be provided in each hour. So, the corrected heating and cooling demand is generated using the assumption that internal building loads can be satisfied with internal mechanisms before relying on the GSHP system. To elaborate, if an hour has a large heating demand and a small cooling demand, the cooling demand can be met by removing heat from the zone requiring cooling and moving it to the zone requiring heating, before calling on the GSHP system. Appendix A contains the corrected heating and cooling loads.

Table 1 – Building GSHP System Details, Courtesy of [4]

	Description
Design Capacity	Peak: 200 tons of cooling
Borehole Configuration	Total Boreholes: 72 Total Branches: 12 Boreholes per Branch: 6
Borehole Material	1.25" SDR11 HDPE – I.D. of 1.34"
Geo-Field Circulation System	2 pumps connected in parallel Model: TACO KV4007 BEP: 600 USGPM, 120' head, 78% efficiency
Circulation Fluid	30% Propylene glycol solution

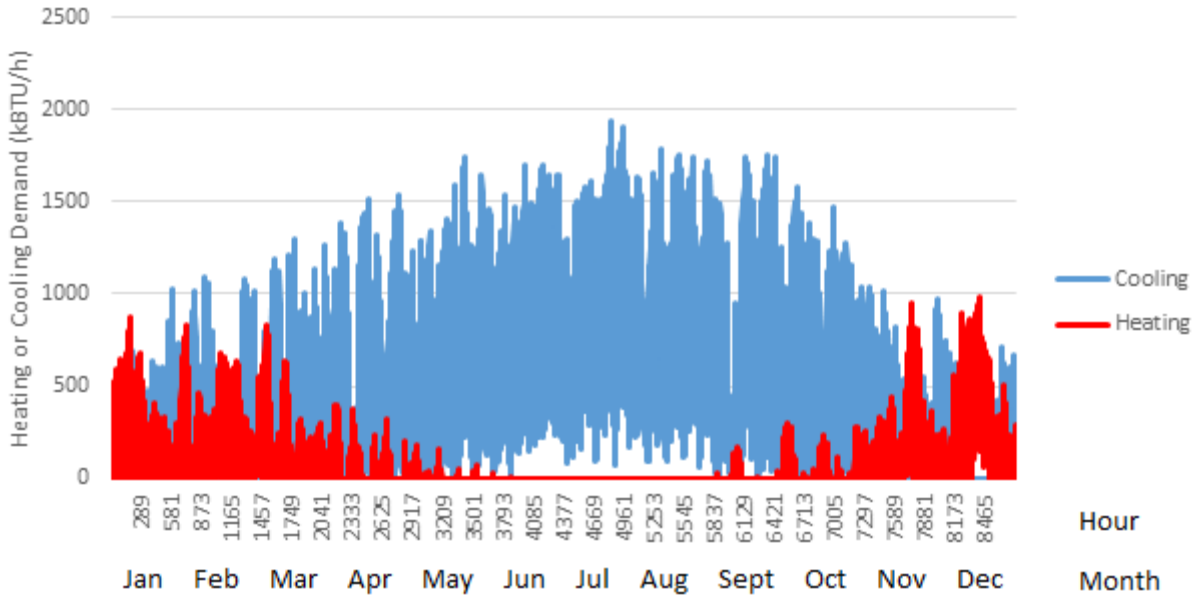

Figure 21 – Hourly Annual Building Heating and Cooling Demand (Corrected)

Table 2 – Hours of the Year Belonging to Each Month

Month	Hours
January	1 – 744
February	745 – 1416
March	1417 – 2160
April	2161 – 2880
May	2881 – 3624
June	3625 – 4344
July	4345 – 5088
August	5089 – 5832
September	5833 – 6552
October	6553 – 7296
November	7297 – 8016
December	8017 – 8760

Figures 22 and 23 show the peak monthly heating and cooling demands, and average daily heating and cooling demands, respectively. Figure 22 shows the maximum hourly heating and cooling load during each month. Figure 23 is the summation of all of the loads in the month, divided by the number of days in that month.

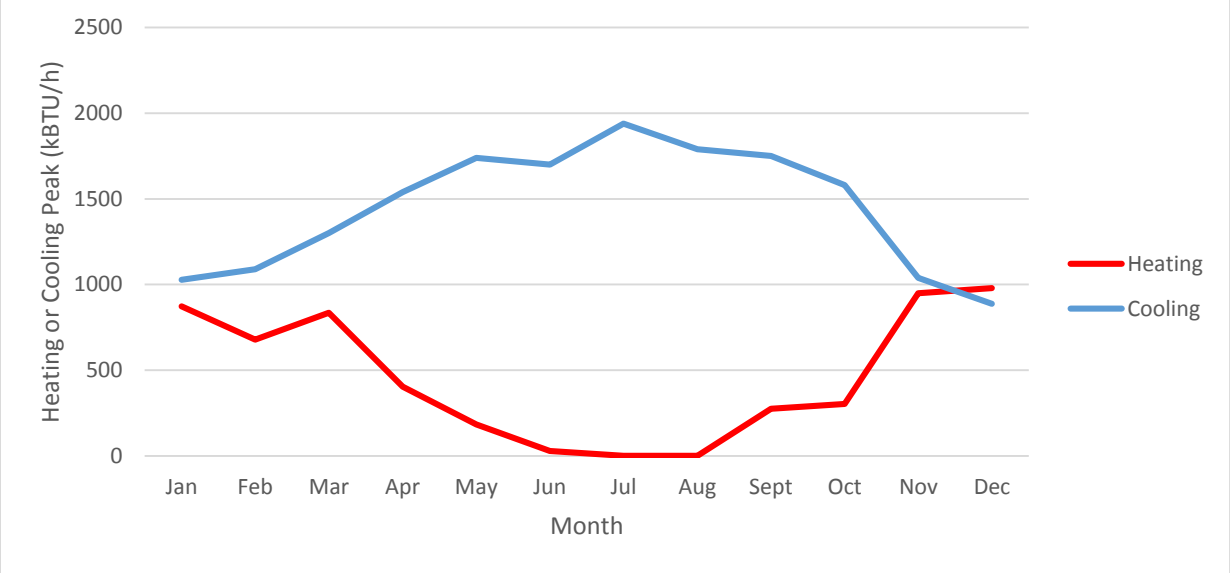

Figure 22 – Peak Monthly Heating and Cooling Demands

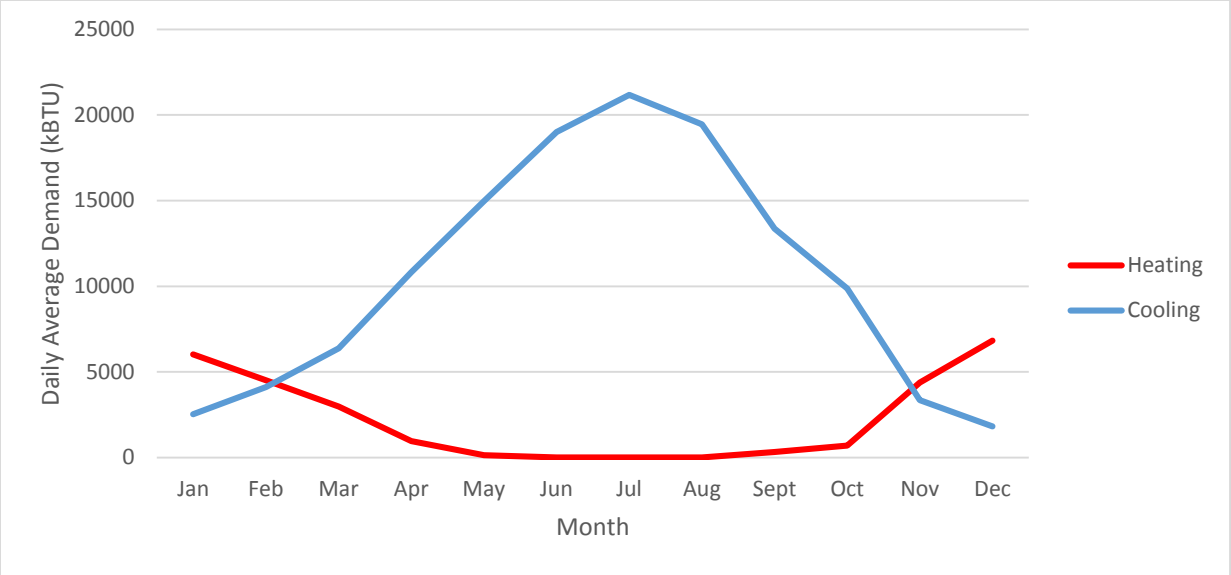

Figure 23 – Average Daily Heating and Cooling Demands

3.3 Base Case, without 'Smart Manifold'

The first case considers a conventional design, without the addition of the 'Smart Manifold'. In this case, the entire geo-field is used, and the flow rate of the circulation pumps must at least be the lowest value for which turbulent flow is created within the boreholes. The fluid temperature that the Reynolds number is evaluated at changes depending on whether the system is in cooling or heating mode. This temperature has been assumed to be 46°F in heating, and 85°F in cooling, as per suggested heat pump inlet design temperature [39].

Figure 24 illustrates the effect fluid temperature has on Reynolds number in each of the 72 boreholes, calculated using Equation 7, based on design information in Table 1 as well as properties in Appendix B. In heating mode, turbulence is achieved at a total system flow rate of nearly 600 USGPM, whereas in cooling mode turbulence begins at approximately 260 USGPM. It is important to note that 600 USGPM is the maximum design flow rate for the pumps chosen for this application, but also the minimum value at which there is turbulent flow in heating mode. The sensitivity of Reynolds number to temperature at a constant flow rate can be seen in Figure 25.

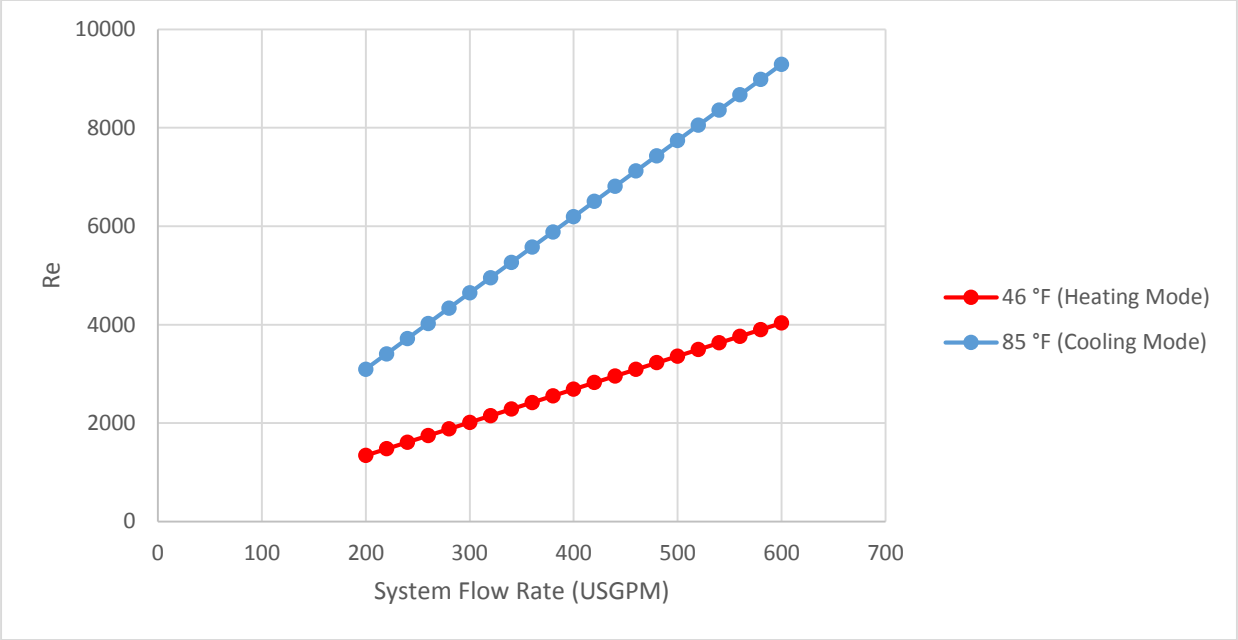

Figure 24 – Effects of Fluid Temperature on Reynolds Number

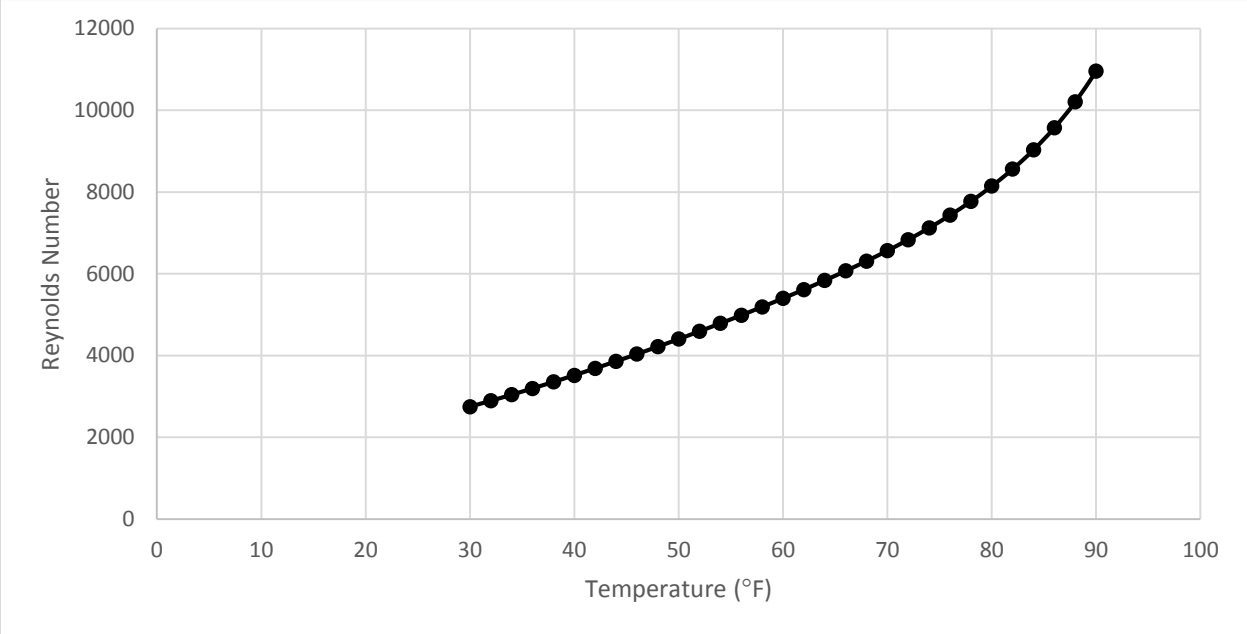

Figure 25 – Sensitivity of Reynolds Number to Temperature at System Flow Rate of 600 USGPM

The next condition that constrains flow is the amount of heat required from the geo-field. From the energy model, and Equation 5, mass flow rate can be calculated. Specific heat and other properties of 30% propylene glycol can be found in Appendix B. For typical design temperature

difference across heat pumps, Groundheat Solar Wind has recommended that a ΔT of 10°F for cooling mode, and 6°F for heating mode should be used. Based on that assumption, mass flow rate can be calculated. It is assumed that the temperature differential remains constant in each mode.

Since hourly data is generated in the energy model, it is assumed that only one of either heating or cooling can occur, even if there is a call for both in a single hour period. Due to the building having multiple climate zones, requiring both heating and cooling simultaneously is possible. To simplify calculations, it is assumed that if the building requires both heating and cooling simultaneously in an hour, the building is able to regulate itself to some degree before relying on the geothermal system. So, for example, if the building requires a large amount of heating and a small amount of cooling during the same hour, the cooling is achieved by extracting heat from the zones needing cooling, which is rejected into the zones requiring heating; the remainder of the load is then supplied by the geo-field.

Using the solved mass flow rates, as well as the corrected heating and cooling load profile from Figure 21, Figure 26 was generated, showing the required circulation pump volumetric flow rate to meet heating or cooling load. Figure 27 represents the percentage of total pump capacity required, and Figure 28 shows the frequency of hourly pump demands.

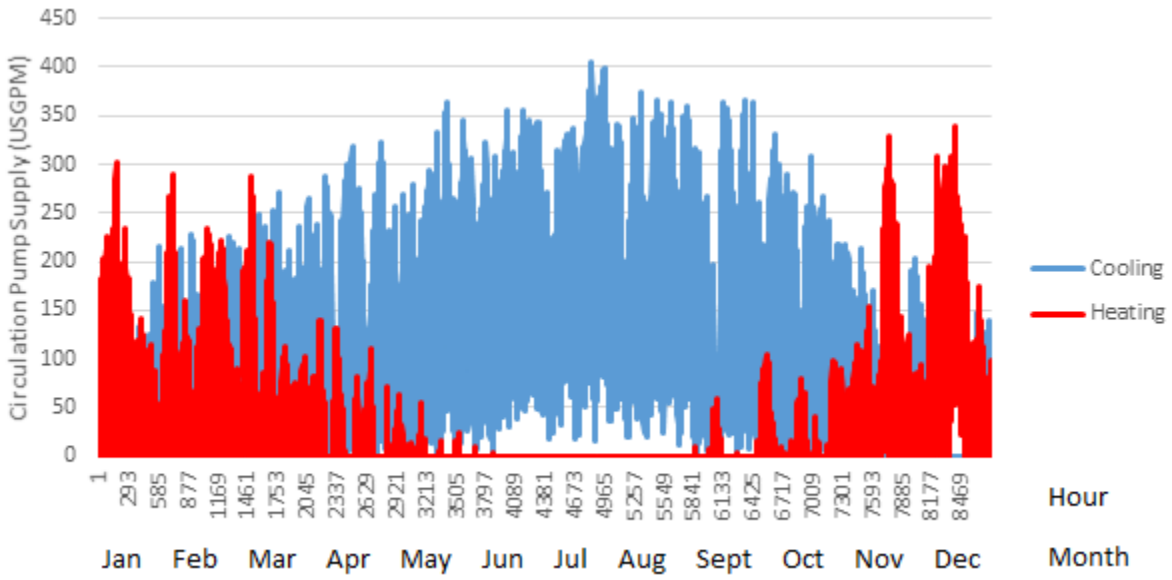

Figure 26 – Hourly Circulation Pump Required Supply

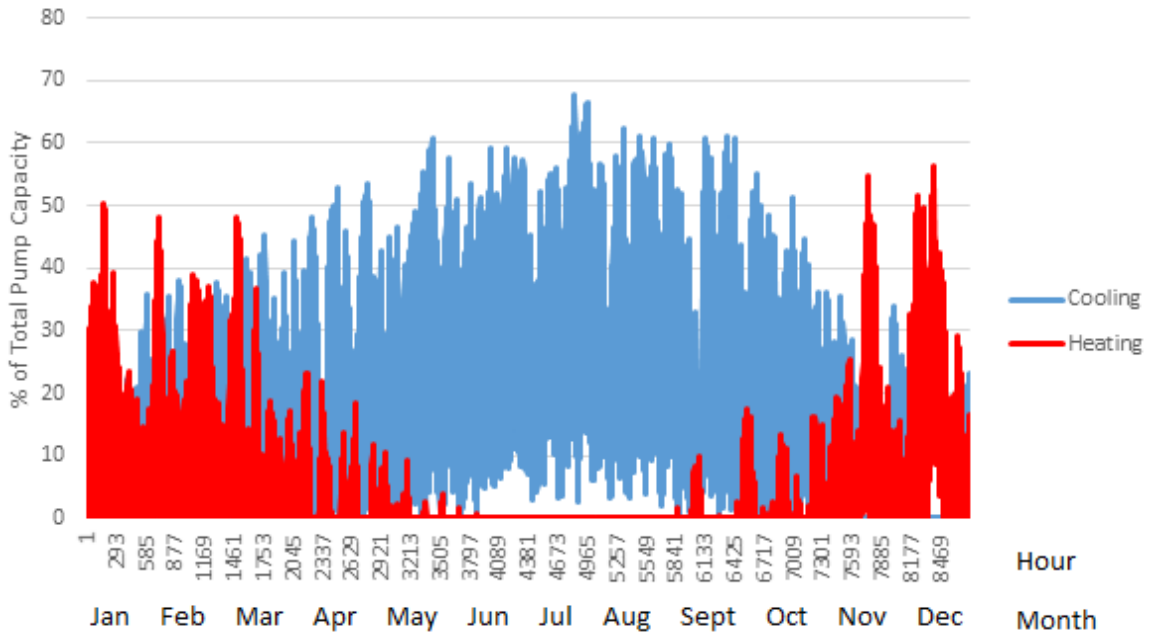

Figure 27 – Hourly Required Circulation Pump Capacity

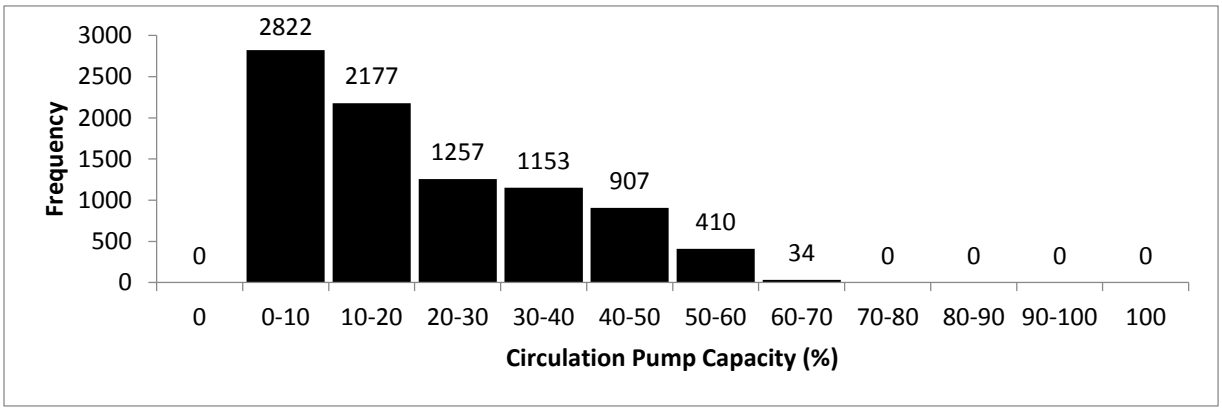

Figure 28 – Yearly Frequency of Circulation Pump Load

From Figure 28, it can be seen that the energy model results in a case where the building calls for heating or cooling every hour of the year. This is a highly unlikely scenario. To correct for this anomaly, it is assumed that during an hour that has a heating or cooling requirement that results in a circulation pump flow rate of under 10% of design circulation pump capacity, the heating or cooling demand value is added to the subsequent hour's demand. Figure 29 is the new histogram for the corrected operation of the GSHP system.

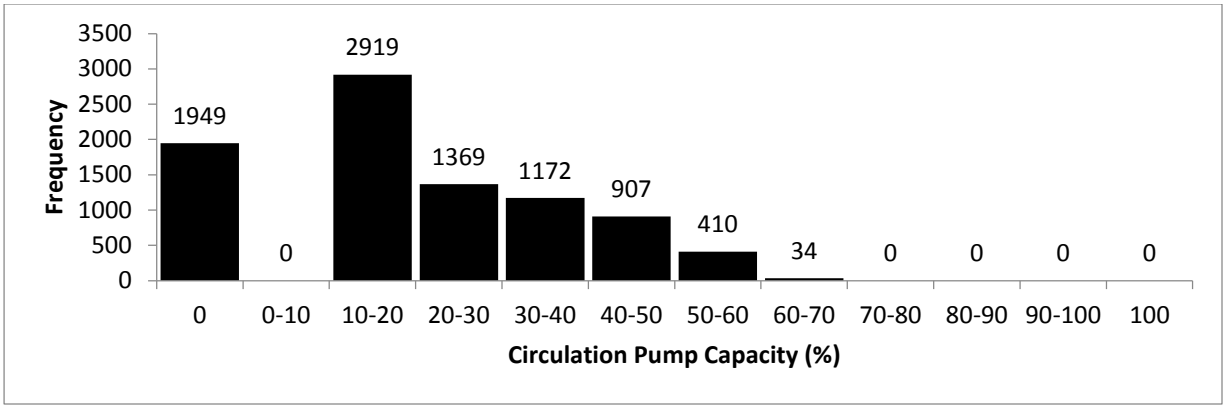

Figure 29 – Corrected Yearly Frequency of Circulation Pump Load

It is clear from Figures 28 and 29 that the circulation pump is oversized for this application, as there is not a single call for the pump to operate above 70% design capacity. It should be noted that energy models consider the average weather patterns when calculating energy requirements, and it is up to the system designers to add a factor of safety for extreme weather, which may explain why the model suggests a low pump capacity.

In addition to determining flow rates required for turbulence and sufficient heat transfer, an upper boundary is required for an acceptable cycle run time. In any household, if the heating or cooling demand takes excessively long to be satisfied, it will cause uncomfortable living conditions. To determine the maximum acceptable run time per call for heating or cooling, the circulation pump capacity was set to 100% for both heating and cooling, and the longest run time was selected. Since the design of a GSHP system takes into account comfort levels of the building's inhabitants, in addition to efficiency, there must be an upper limit to how long it takes to satisfy building demands. As a result, the longest time it takes the system to meet demand conditions while running at full circulation pump capacity is assumed to be the longest acceptable run time for all cases.

3.4 Addition of 'Smart Manifold'

Since the circulation pump demand is very low for the majority of the year, but high flow rates are required to maintain turbulence, a conflict arises between pump operation and heat transfer efficiency. With the addition of the 'Smart Manifold', the system is no longer constrained by the requirement to maintain high total system flows required for turbulence. A schematic of the 'Smart Manifold' is shown in Figure 30. Figure 30 is a modification of one of the manifolds to

include solenoid valves that would be programmed into the building's control logic. Figure 30 differs from Figure 18, not only due to the addition of actuated valves, but also in the addition of lines coming into the manifold. Figure 18 represented a general schematic, whereas Figure 30 is representative of the case being investigated for the purposes of this thesis, which has a total of 12 branches, as opposed to Figure 18's 6 branches.

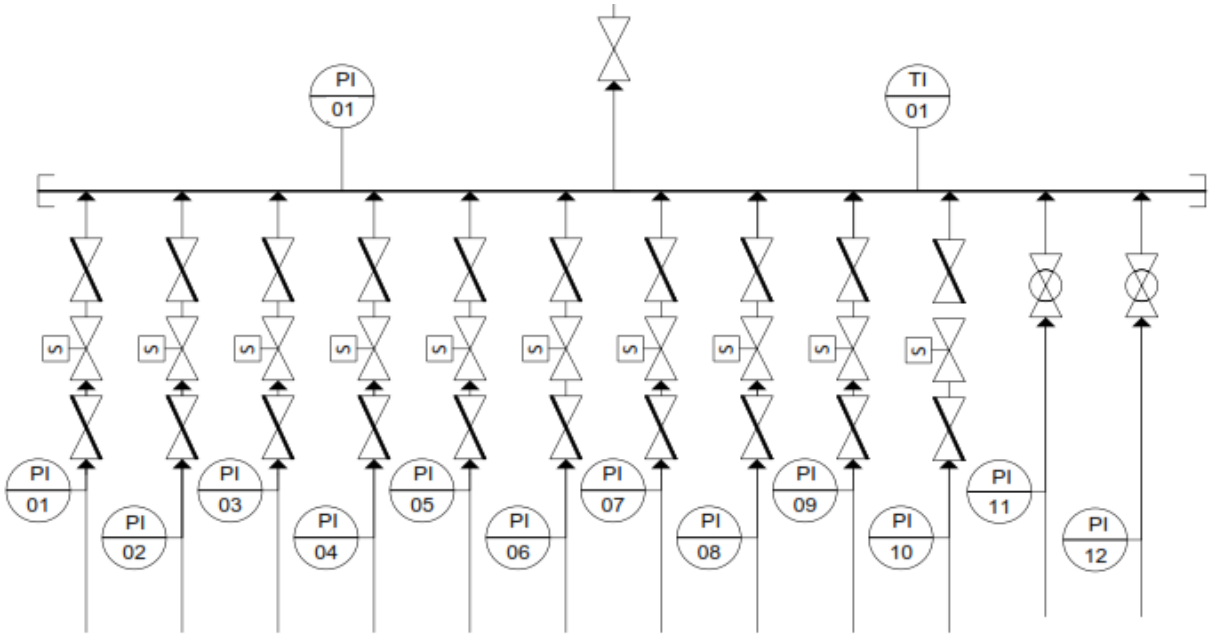

Figure 30 – 'Smart Manifold' Modification

The assumption being considered is that in any GSHP system, effective heat transfer must be supplied in a timely manner. So, it is assumed that the minimum allowable flow rate ensures turbulence, and the heating or cooling load must be satisfied within the maximum time for the 100% circulation pump design capacity case. For the no 'Smart Manifold' case, the lowest pump capacity required for turbulence is set, and the run time is calculated. If the run time exceeds the maximum allowable duration, the run time is set to the maximum and the flow rate is calculated. By this method, both time and flow conditions are met.

In the case with a 'Smart Manifold', the geo-field is scalable due to the addition of the actuated valves on the branches coming into the manifold. By scaling the geo-field, thereby isolating certain branches, the flow is divided amongst fewer branches. As a result, a reduced flow

paired with a smaller geo-field will lead to maintenance of high flow within the boreholes. Consider the modification of Equation 2:

$$Q_{Total} = Q_{branch\,1} + Q_{branch\,2} + \cdots + Q_{branch\,n}$$

and,

$$Q_{branch\,1} = Q_{branch\,2} = \cdots = Q_{branch\,n}$$

so,

$$\frac{Q_{Total}}{n\ branches} = Q_{branch\,1} = Q_{branch\,2} = \cdots = Q_{branch\,n}$$

Therefore, high flow rates in active branches can be maintained while system flow rate and power consumption are reduced. Figure 31 shows the relationship between flow rate and Reynolds number at 100% and 50% geo-field size. The ability for the geo-field to be scaled, however, is not infinite. Rather, it is limited to step intervals defined by the number of branches in the system.

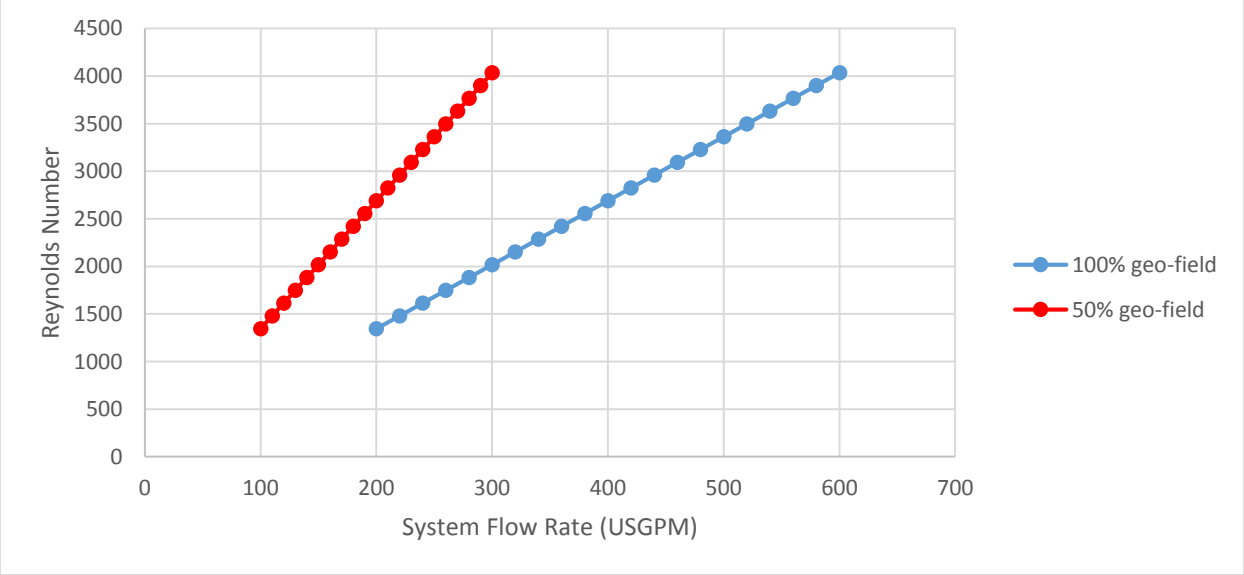

Figure 31 – Reynolds Number at Varying Geo-Field Size, with Fluid Temperature at 46°F

So, instead of fixing the flow rates and calculating run time like in the no 'Smart Manifold' case, the 'Smart Manifold' case sets the longest acceptable time and calculates the required flow, and the corresponding geo-field size. The next chapter considers the potential energy savings with the 'Smart Manifold'.

Chapter 4 – Results

4.1 Case I – Establishing Maximum Acceptable Run Time (no 'Smart Manifold')

Case I is used to set the maximum acceptable run time in order to meet building demands in a timely manner, and does not include the 'Smart Manifold'. This case sets pump flow rate to 100% design capacity and selects the maximum pump run time as the longest acceptable for future cases. This case also provides a basis for comparison for the 'Smart Manifold' analysis. The longest run time is found by using Equations 5 and 6 in Chapter 3, along with the building energy simulation data. Utilizing Equation 5, the mass flow rate required to meet the heating or cooling demand can be solved. Then, Equation 6 allows for volumetric flow rate to be solved. The volumetric flow rate calculated at this point is the minimum possible to provide the required heat transfer, taking a full hour. However, Case I will use the circulation pump's maximum flow rate of 600 USGPM. So, by dividing the minimum flow rate required by the maximum, the result is the percentage of an hour at which the pump must run at maximum capacity to supply the same volume of fluid. For Case I, the maximum run time is 40.55 minutes. This value is used as the maximum allowable cycle run time to ensure building comfort, as described in Chapter 3. The hourly cycle time throughout the year can be seen in Figure 32. Maximum and average monthly run time is also important to note, and can be seen in Figures 33 and 34, respectively. Comparing Figures 33 and 34 shows a clear disparity between maximum and average run times. In fact, the average run time is merely 12.45 minutes compared to the 40.55 maximum. Short cycles should generally be avoided, since running for durations longer at reduced capacity offers the benefit of energy savings as well as a reduction in mechanical wear [36]. Running a GSHP system will affect the ground temperature, and short cycling inhibits the fluid in the loop from equilibrating with the ground temperature during the cycle run time. Large differences in inlet temperatures to the heat pump are associated with a reduction in heat pump COP [40]. The study showed that shorter run times resulted in higher heat pump COPs. The reason for this is that the fluid at the heat pump inlet was all previously at rest within the ground loop, and thus an even temperature throughout. Conversely, at longer run times the heat pump's outlet fluid, which is at a different temperature than the inlet fluid, will have sufficient time to pass through the ground loop and return to the heat pump inlet, without being at rest long enough to equalize with ground temperature.

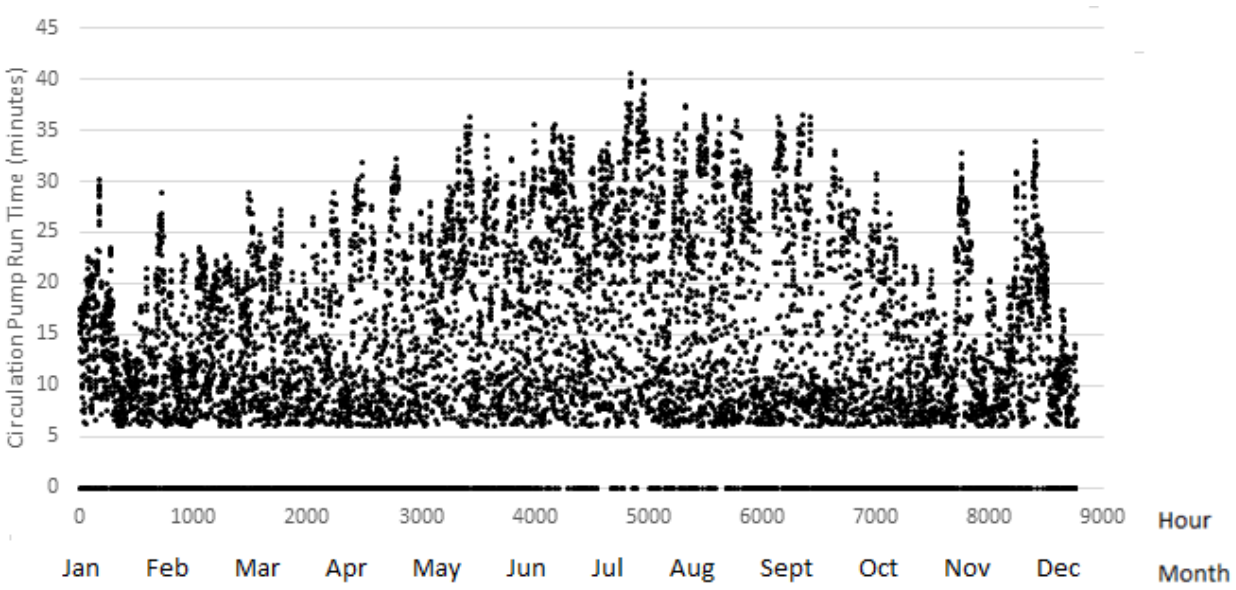

Figure 32 – Case I, Circulation Pump Run Time at Full Capacity

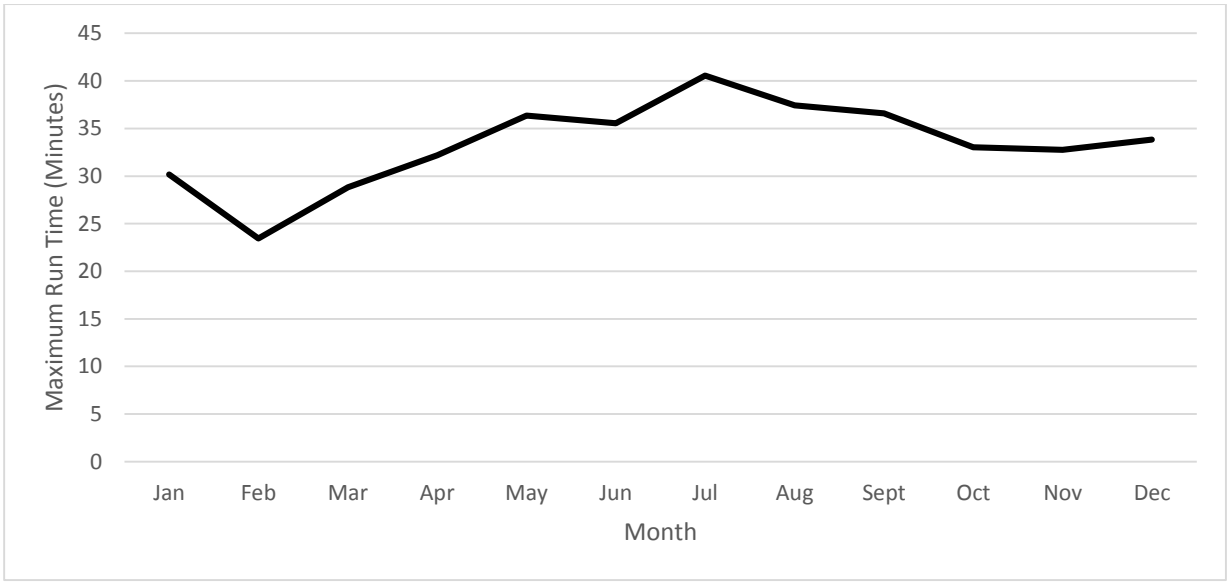

Figure 33 – Case I, Circulation Pump Hourly Maximum Run Time by Month

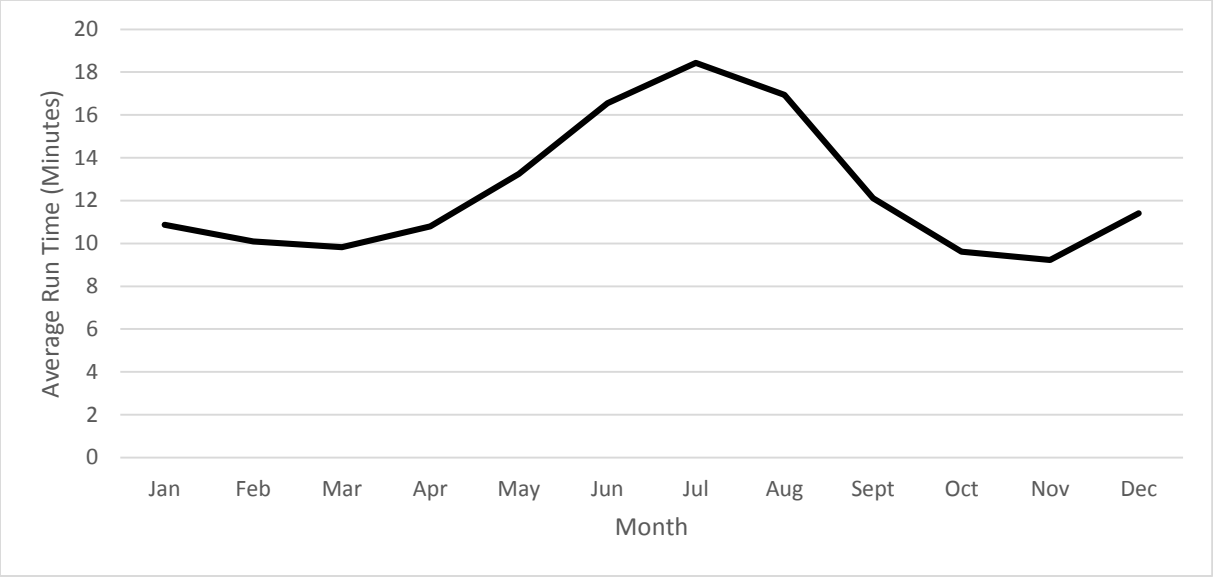

Figure 34 – Case I, Hourly Average Circulation Pump Run Time by Month

Case I is used primarily to set a baseline for cycle run times, but it is also advantageous to calculate the power consumption based on current design techniques. By comparing power consumption in each of the cases, a clearer progression of the power savings can be seen. Pump power is expressed by Equation 9 [34] as:

$$P = \frac{H \times g \times \rho \times Q}{n} \tag{9}$$

H = pump head (ft)

g = acceleration due to gravity (ft/s^2)

n = pump efficiency

Taking pump design conditions for head, flow rate and efficiency from Table 1, and the average density of the fluid based on properties in Appendix B, Equation 9 gives:

$$P = \frac{(120\ feet) \times (32.174\ ft/s^2) \times (64\ lb/ft^3) \times (600\ USGPM)}{0.78}$$

$$P = 23.95\ BHP = 17.86\ kW$$

The electricity consumption is found by multiplying the power consumption with the run time, and is summarized in Figure 35. With an assumed blended rate of electricity costing $0.17/kWh [39] in Ontario, Canada, the total electricity consumption of the circulation pumps can be calculated. Table 3 summarizes Case I simulation details.

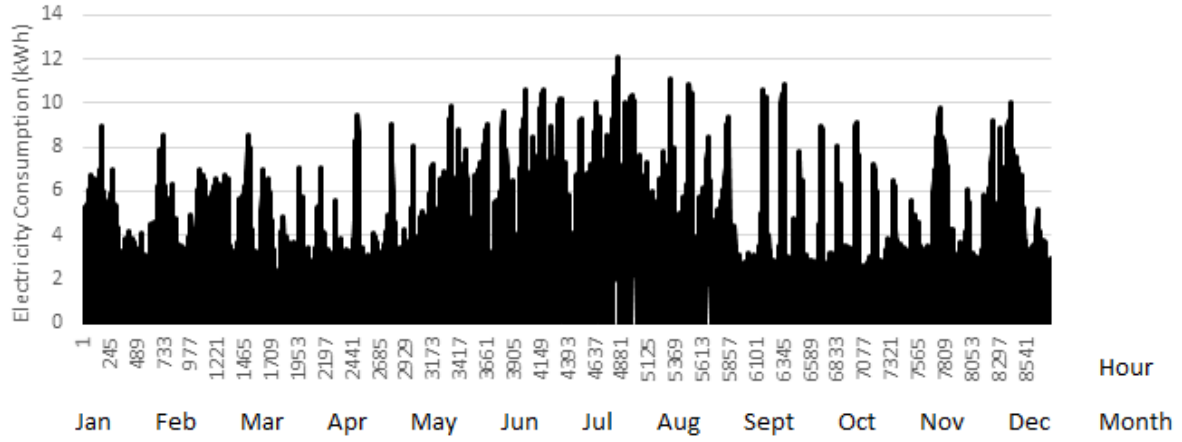

Figure 35 – Case I, Hourly Electricity Consumption

Table 3 – Case I Results Summary

Average Hourly Run Time	12.45 minutes
Maximum Hourly Run Time	40.55 minutes
Average Pump Load	77.75%
Total Yearly Run Time	1817.87 hours
Total Yearly Electricity Use	32467.19 kWh
Total Yearly Electricity Cost	$5519.42

4.2 Case II –Minimum Flow for Turbulence (Without 'Smart Manifold')

In Case II, the circulation pump is set to the lowest value at which turbulent flow is achieved in the ground loop without the 'Smart Manifold'. If the run time at that capacity exceeds the maximum assumed run time of 40.55 minutes, the run time for that hour of the year is set to 40.55 minutes and the required increased pump capacity is calculated to meet the heating or cooling demand in that time. Since turbulence in the heating mode only occurs when the circulation pump operates at full capacity, the savings in this case are a result of scaling down the pump during

the cooling mode, when turbulence occurs at much lower pump speeds, as illustrated by Figure 24. Figure 36 shows the pump run time for Case II, and Figure 37 shows the average monthly run time. The corrected pump capacities are shown in Figure 38, which is used in the calculation of electricity consumption in Figure 39. From Equation 4, pump power consumption is calculated as the cube of speed. For example, a speed reduction of 50% results in a power consumption reduction of a factor of eight. Also run times are more consistent in Figure 36 in comparison to Figure 32 for Case I.

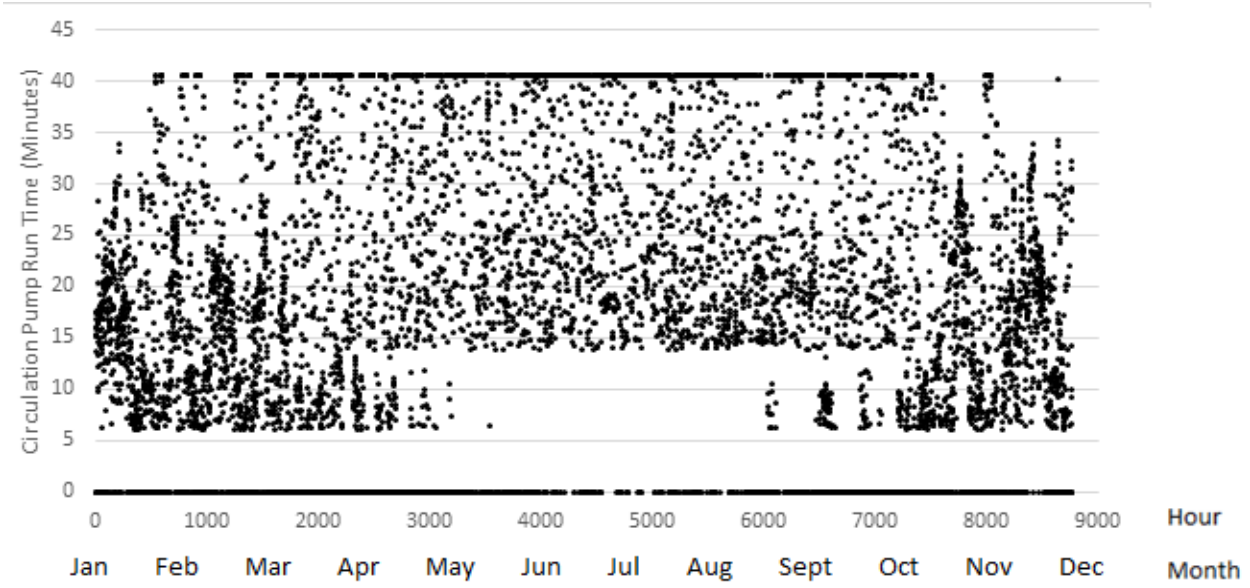

Figure 36 – Case II, Hourly Pump Run Time, Lowest Turbulent Flow (Without 'Smart Manifold')

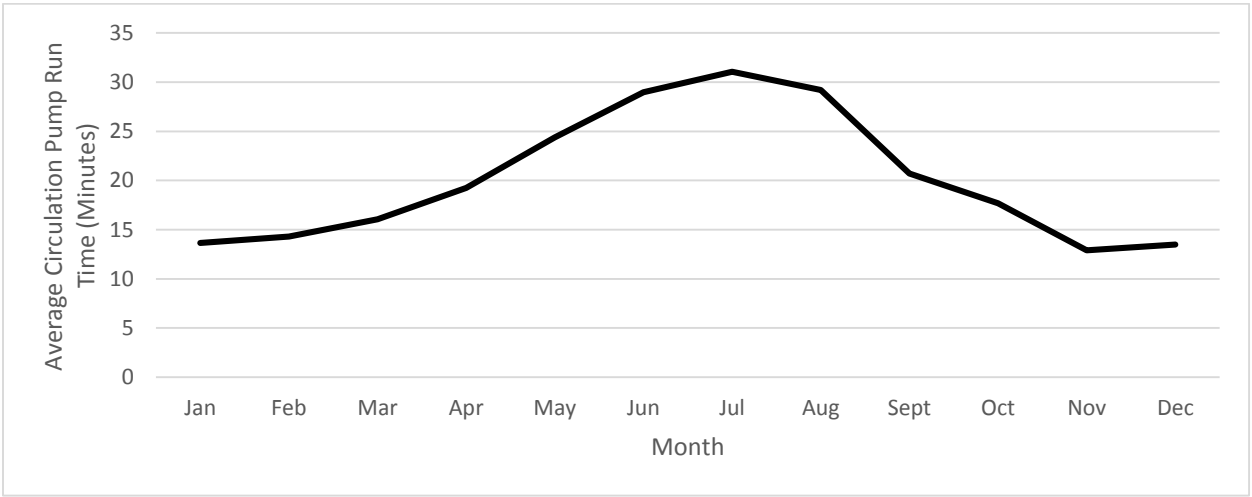

Figure 37 – Case II, Average Hourly Circulation Pump Run Time by Month

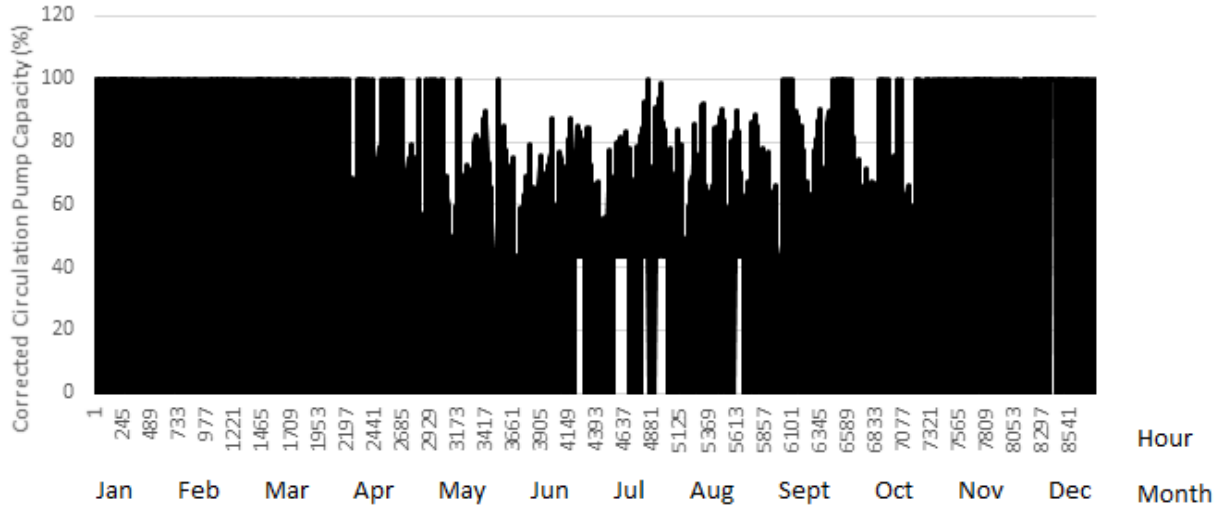

Figure 38 – Case II, Hourly Pump Capacity

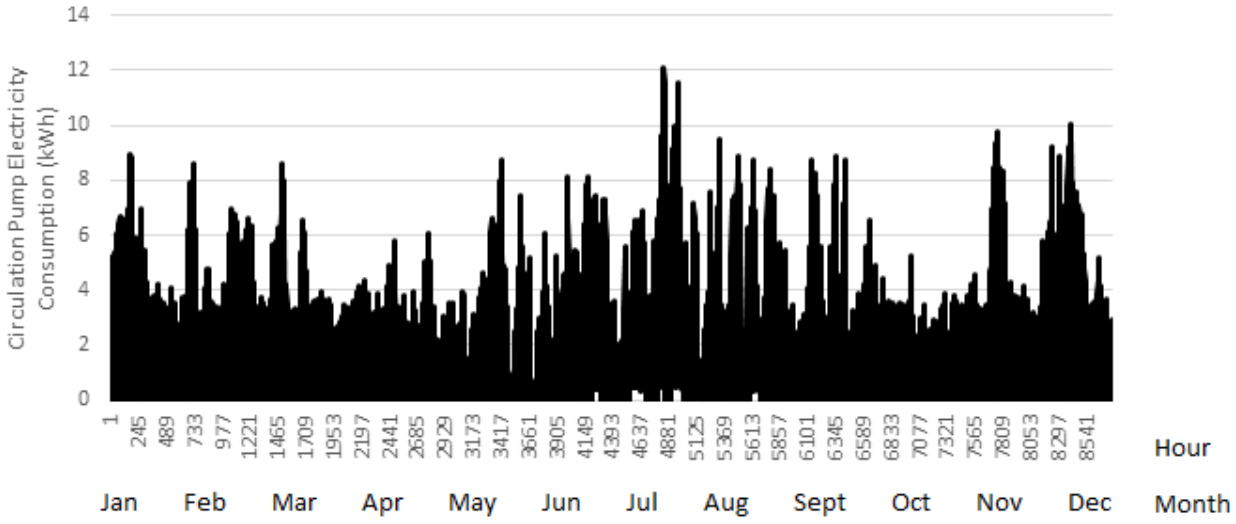

Figure 39 – Case II, Circulation Pump Electricity Consumption

In Figure 29, the yearly frequency of circulation pump load was shown for the hypothetical case where pump flow was not restricted by the requirement to supply turbulent flow. Figure 40, however, shows the frequency of pump load with the added condition of maintaining turbulence. It is clear that Figures 29 and 40 are drastically different, which illustrates that Case II must maintain high levels of pump loading to consistently provide turbulent flow. High levels of circulation pump loading inadequately takes advantage of the VFD's ability to provide energy savings, as will be seen by the 'Smart Manifold' scenario in Case III.

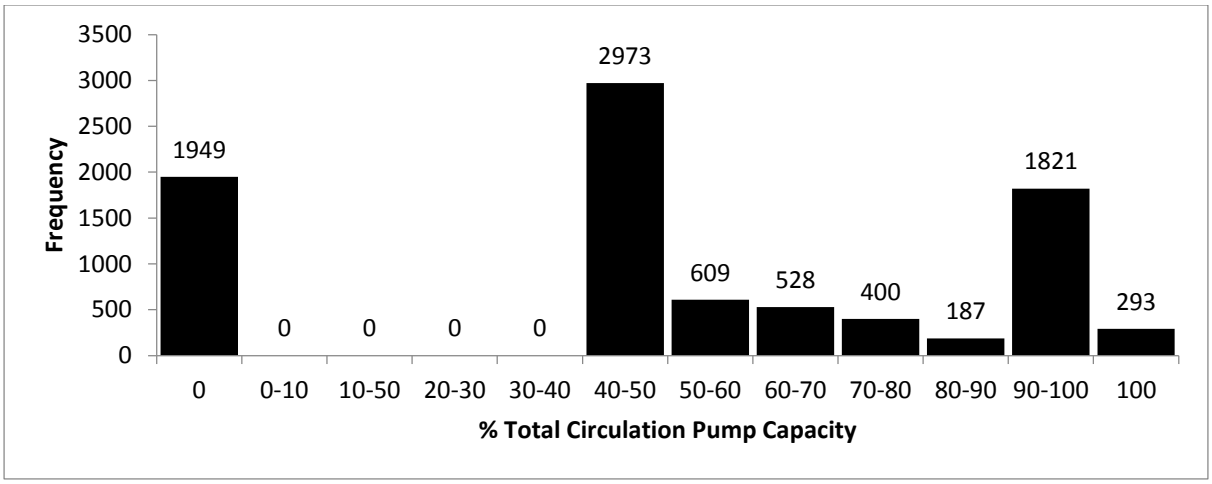

Figure 40 – Case II, Yearly Frequency of Circulation Pump Load

Table 4 summarizes the results from Case II. Notable improvements from Case I include longer average hourly run time, reduced average pump capacity, and a large reduction in electricity use. A possible disadvantage of Case II is that Case I has must higher flow rates during the cooling mode. While both cases remain turbulent at all times, Case I has a much higher level of turbulence, and thus a higher rate of convective heat transfer.

Table 4 – Case II Results Summary

Average Hourly Run Time	20.18 minutes
Maximum Hourly Run Time	40.55 minutes
Average Pump Load	51.87%
Total Yearly Run Time	2946.87 hours
Total Yearly Electricity Use	16884.60 kWh
Total Yearly Electricity Cost	$2870.38

4.3 Case III – 'Smart Manifold' Implementation

As mentioned in Chapter 3, the Smart Manifold endeavors to keep the system run time high, within the limitations of turbulent ground loop flow and occupant comfort. Longer average run times correspond to a reduction in average pump capacity, which in turn leads to reduced energy consumption, decreased mechanical wear, and decreased effects of short cycling. Circulation pump run times in Case III, shown in Figure 41, are more consistent than in the

previous cases. Figure 42 shows the comparison between hourly pump run times in Cases II and III in the first week, or 168 hours.

As there are a finite integer number of ground circulation loops in a given system, the 'Smart Manifold' is not infinitely variable, so the geo-field is limited in its ability to match every required capacity. For the building in this case study, the geo-field is divided into 12 branches, which results in intervals $\frac{1}{12}$ of the total geo-field capacity. So, the calculated minimum pump capacity is rounded up to the nearest setting that the 'Smart Manifold' can achieve. Figure 43 illustrates the small disparity between the minimum and corrected pump loads. Corrected pump loads are calculated based on the size of the geo-field, as set by the 'Smart Manifold'. Compared to Case II, Case III utilizes less energy annually, despite longer run times. Energy consumption for Case III is shown in Figure 44.

The 'Smart Manifold' will require the addition of solenoid valves to the header pipes entering one of the manifolds. Only one manifold requires actuated valves, since closing one end of the loop will cause a pressure build up that stops the flow at the other end. The other components required for a properly functioning 'Smart Manifold' are the VFDs on each pump, as well as temperature sensors on each manifold. However, typical GSHP designs include VFDs and a multitude of sensory devices. It is assumed that the only additional equipment required will be solenoid valves. The life of the solenoid valves is assumed to be equal to the life of the entire GSHP system, 20 years. The power consumption and maintenance of the valves is assumed to be negligible for the purposes of cost calculations.

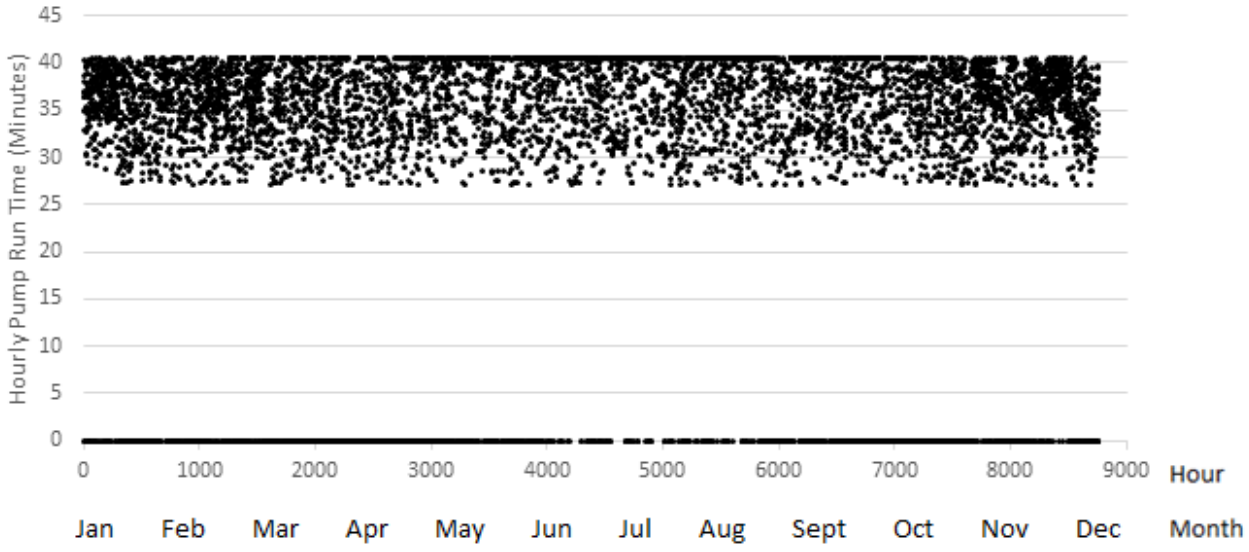

Figure 41 – Case III, Hourly Pump Run Times

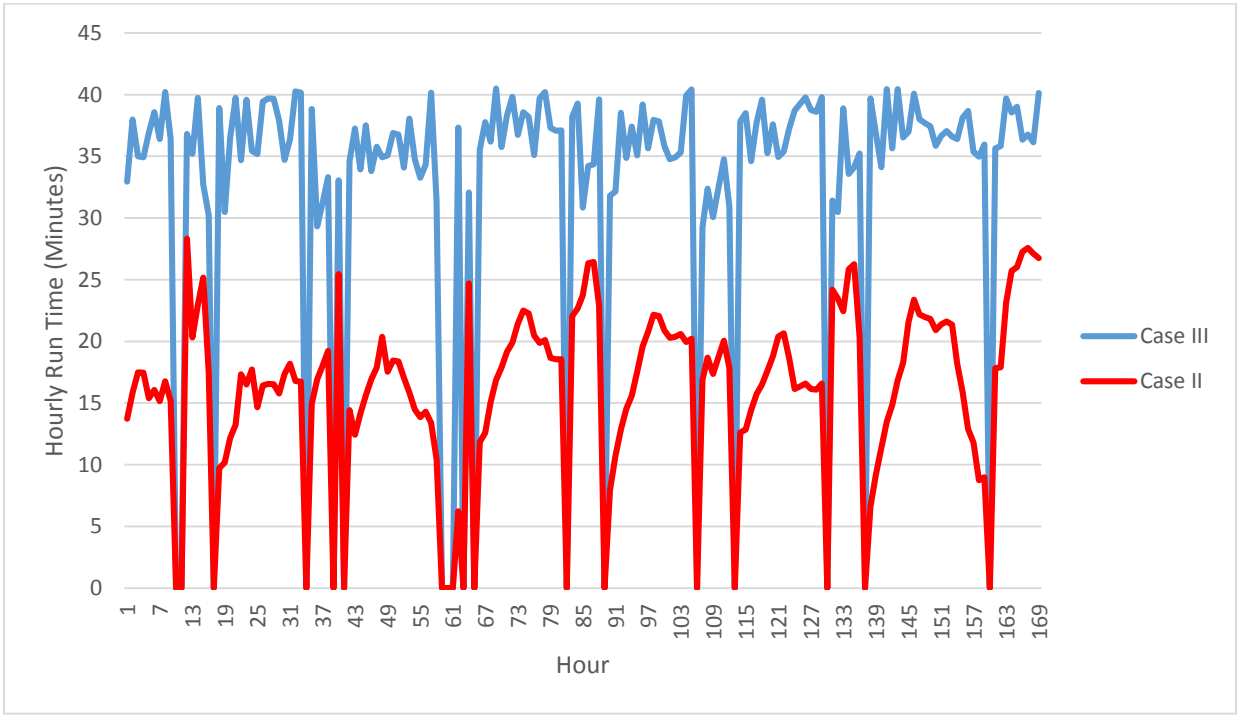

Figure 42 – Hourly Run Time for Cases II and III

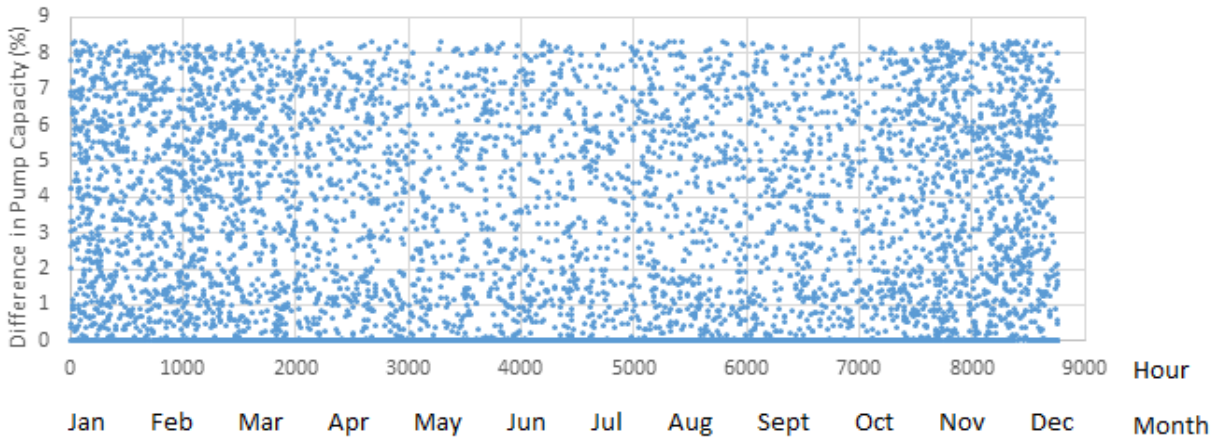

Figure 43 – Case III, Difference in Minimum vs. Corrected Pump Load

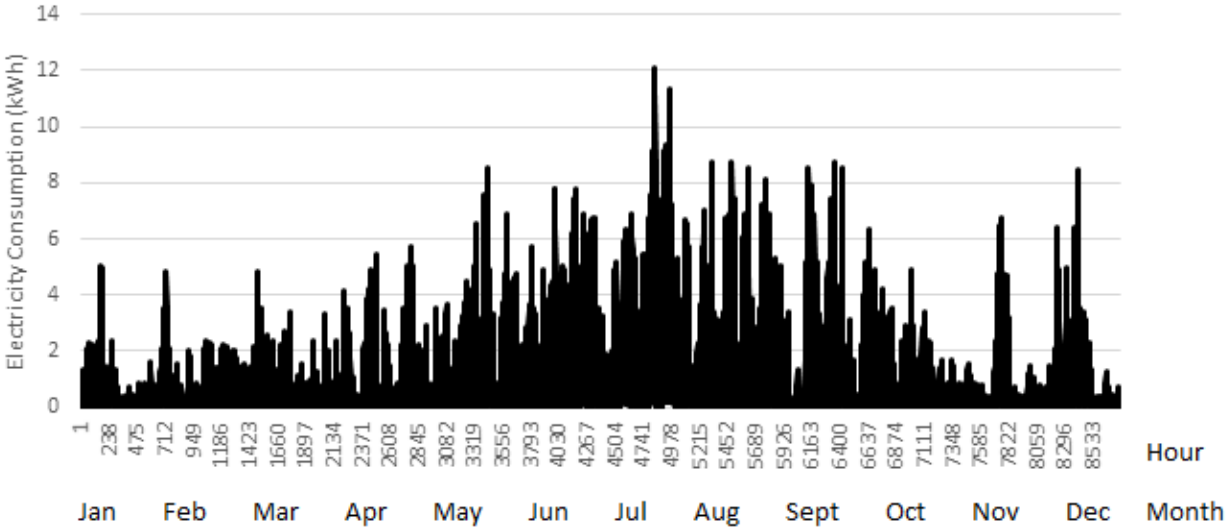

Figure 44 – Case III, Hourly Pump Electricity Consumption

The histogram in Figure 45 shows frequencies of pump loading throughout the year for Case III. Figure 45 has a frequency distribution that more closely resembles the histogram in Figure 29 as compared to its resemblance in Figure 40 for Case II. Since Figure 29 is the histogram for the hypothetical case where maintaining turbulence is not a factor in pump loading, the flow capacities are as low as possible while still meeting heating or cooling requirements.

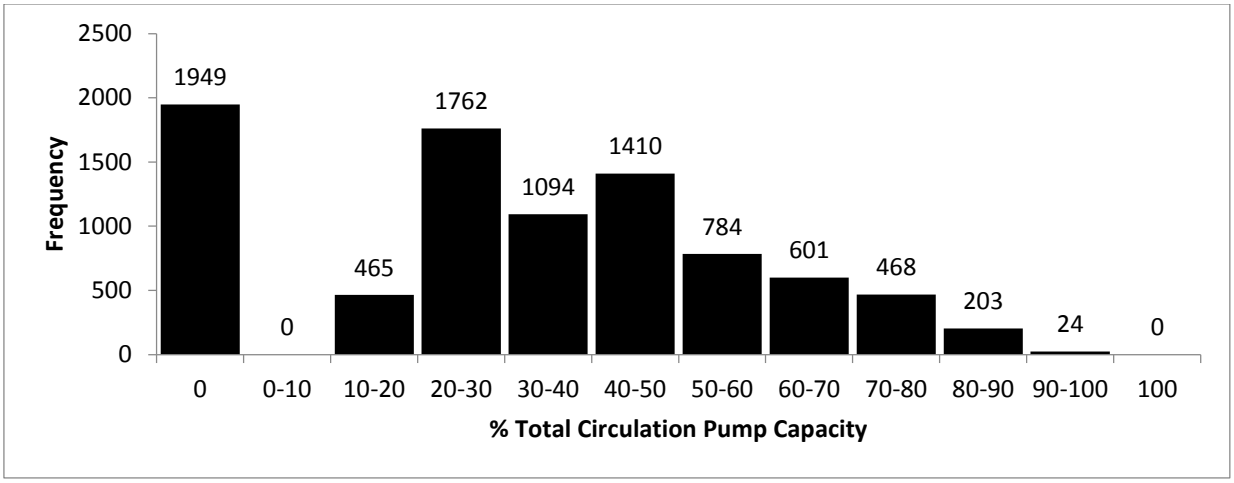

Figure 45 – Case III, Yearly Frequency of Circulation Pump Load

The results of Case III are summarized in Table 5. Despite longer run times than either of the no 'Smart Manifold' cases, Case III still consumes less electricity because the pump operates at a lower rate. Figure 46 shows the difference in electricity cost between Case II and Case III. Figure 47 shows the frequency of the number of closed branches. The 42% reduction in geo-field circulation pump electricity consumption is due to the reduced average pump capacity of 32.87% compared to 51.87% in Case II.

Table 5 – Case III Results Summary

Average Hourly Run Time	31.53 minutes
Maximum Hourly Run Time	40.55 minutes
Average Pump Load	32.87%
Total Yearly Run Time	4191.45 hours
Total Yearly Electricity Use	9763.15 kWh
Electricity Saved Compared to Case II	7121.45 kWh
Total Yearly Electricity Cost	$1659.74
Total Yearly Electricity Cost Savings Compared to Case II	$1210.65

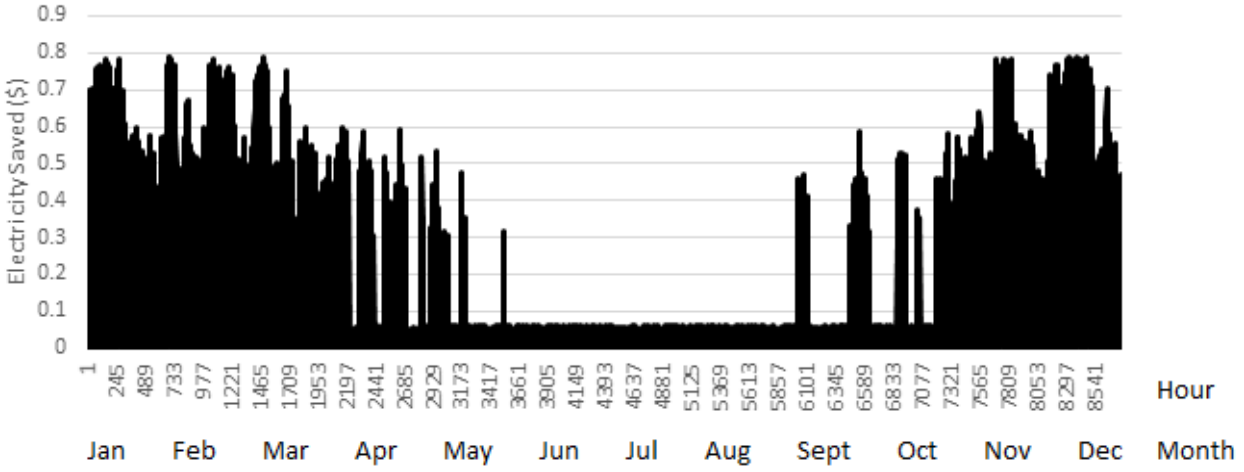

Figure 46 – Electricity Saved Between Case II and Case III

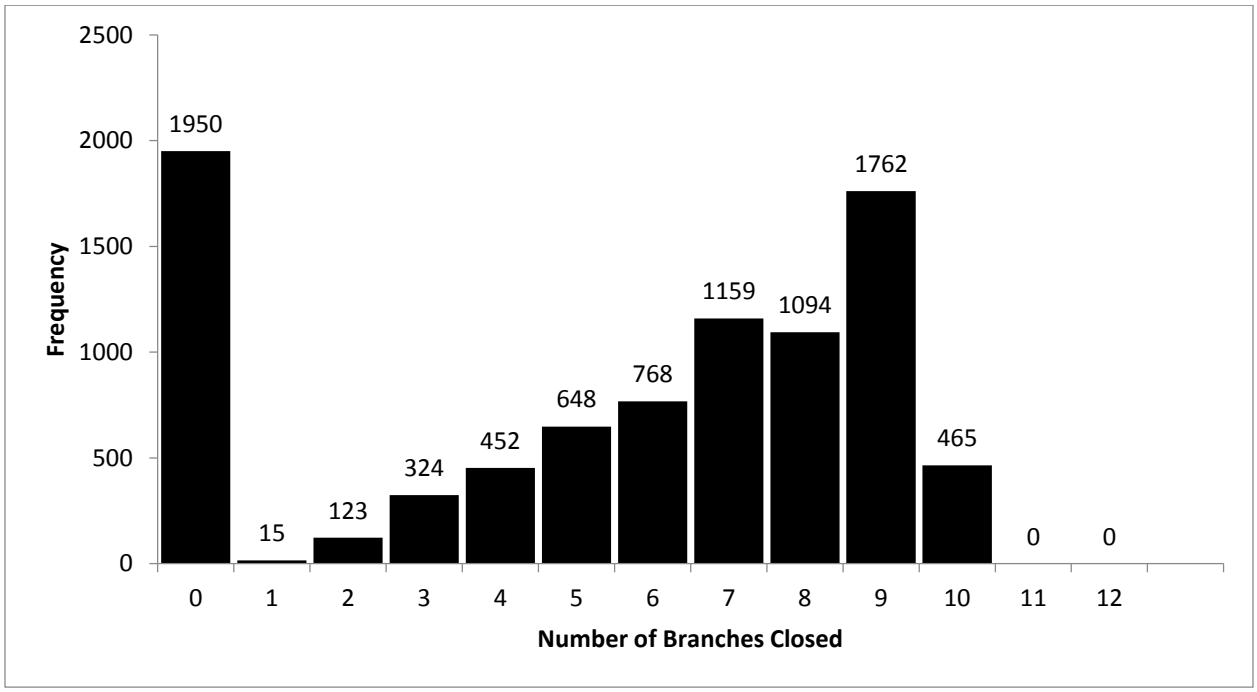

Figure 47 – Frequency of Branches Closed

4.4 'Smart Manifold' NPV, Payback Time and Emissions Saved

For the 'Smart Manifold' to be feasible, it must have a reasonable payback period. GSHP systems as a whole typically have payback periods that range from 7 - 12 years, or more, as discussed in Chapter 2. While the 'Smart Manifold' will increase capital costs, it will decrease overall system payback. The payback time for the overall system and for the 'Smart Manifold' are

examined separately. A payback time for a 'Smart Manifold' of 7 or fewer years would be a worthwhile investment. For a retrofit installation of a 'Smart Manifold' in an existing GSHP system, a shorter payback period would be expected, depending on the remaining life of the existing GSHP installation.

According to Groundheat Solar Wind, the cost of actuated valves sometimes increases exponentially with size [4]. In other words, a solenoid valve that is twice the size of another one may be more than double its price. To reduce the cost of materials, Mr. Di Rezze, P.Eng., of Groundheat Solar Wind suggested using a smaller solenoid valve accompanied by pipe reduction immediately before the valve, and an expansion immediately after. The pipes used in the vertical boreholes in this case study are 1.25" in diameter. However, the header pipes entering the manifold are between 2" and 3" in diameter due to the number of boreholes being collected into a branch. So, rather than using a larger and more expensive 2" solenoid valve, it may be possible to use a 1.25" valve in order to reduce material cost. According to Mr. Esmail of Groundheat Solar Wind, the total cost of one 1.25" solenoid valve is $418.44, while the 2" valve costs $725.88. The assumption of using a 1.25" valve is reliant on the assumption that the increase in pressure due to the reduction in pipe diameter is within the valve's design operating pressure. It is assumed that the increase in pressure drop from adding the reduction and smaller valves is negligible in terms of additional pump power. For Case III in Section 4.3, a total of 10 solenoid valves are needed to produce the required level of control, as depicted in Figure 30 in Chapter 3.4.

Electricity rate increases are also important to consider for payback calculations. According to the Ontario Energy Board, off-peak, mid-peak, and on-peak electricity rates from May 2006 to May 2014 increased by 53.3%, 33.0%, and 22.2%, respectively [41]. The increases correspond to yearly average increases of 6.6% for off-peak, 4.1% for mid-peak, and 2.8% for on-peak. These values, however, only consider the increase in electricity cost, without including the increases in charges for administration, distribution, transmission, and other miscellaneous fees. Other sources predict a rise 33% over the next three years in Ontario, as a result of government energy plans [42]. For the purposes of this case study, an average annual increase of 8% is applied to electricity costs. Table 6 is a summary of variables used in NPV and payback calculations.

Table 6 – Variables for NPV and Payback Calculations

Scenario 1: Cost per 1.25" Solenoid Valve, Misc. Parts, Installation (includes 13% HST Tax)	$418.44
Scenario 2: Cost per 2" Solenoid Valve and Misc Parts, Installation (includes 13% HST Tax)	$725.88
Number of Solenoid Valves Required	10
Total Cost for Scenario 1	$4184.40
Total Cost for Scenario 2	$7258.80
Annual Energy Savings	$1210.65
Assumed Annual Increase in Electricity Cost	8%
Assumed Annual Discount Rate	8%
Assumed Project Life	20 years

Case III with the addition of the 'Smart Manifold' has two design scenarios. For Scenario 1, shown in Table 6, which uses the 1.25" solenoid valves, the discounted payback period for just the 'Smart Manifold' is 3.73 years, with an NPV of $18,234.98. Scenario 2, which uses 2" solenoid valves, also shown in Table 6, has a much longer discounted payback period for the 'Smart Manifold' of 6.47 years, and a smaller NPV of $15,160.60. Both scenarios have a positive NPV, which suggests a good investment over the life of the project. The discounted payback periods meet the conditions for being financially feasible for new GSHP projects, but may be too long to be considered for retrofit projects. The effect of the 'Smart Manifold' on the payback of an entire GSHP system as a whole, however, is negligible. The total cost for the installation of the entire GSHP system of the same size as the one used for this thesis, without the 'Smart Manifold', is likely to be approximately $1,000,000 or above, according to Groundheat Solar Wind. As a result, a 'Smart Manifold' has very little influence on reducing payback time on the GSHP system as a whole.

In addition to financial savings, the implementation of a 'Smart Manifold' is responsible for the reduction of harmful emissions. According to Dworkin *et al.* [39] in their Geo-Cities Initiative report, every kWh of electricity produced in Ontario is responsible for approximately 0.3 kilograms of carbon dioxide being produced. Since the 'Smart Manifold' in Case III saves 7121.45 kWh compared to Case II, it potentially eliminates the production of 2143.56 kilograms of carbon

dioxide annually. According to reports, 25,000 geothermal heat pumps were installed between 2008 and 2010 in Ontario alone [43], so the savings of carbon emissions from the ‘Smart Manifold’ in every installation in Ontario is potentially very great.

Chapter 5 – Conclusions and Future Work

The ‘Smart Manifold’ has been presented in this thesis as a potential method to increase GSHP system efficiency on the geo-field circulation side, providing financial and environmental benefits. The added control of the geo-field branches allows for the system to save pumping energy without sacrificing thermal efficiency in the vertical boreholes. The methodology investigated a cooling dominant high-rise residential building in Toronto, Ontario, Canada. Based on the assumed design variables, payback time for the ‘Smart Manifold’ system for this case study was found to be between 3.73 and 6.47 years. The payback time calculated is less than or approximately equal to the typical payback period estimate for a full GSHP installation. However, for the purposes of retrofitting existing buildings, the payback period may be too long, depending on the remaining life of the existing installation.

High savings were attained in months where heating was required. In heating mode, fluid temperatures drop to a point at which viscosity significantly impedes the formation of turbulent flow patterns, causing a thermal boundary layer in the pipes, and reducing the efficacy of heat transfer. As a result, the ‘Smart Manifold’ played a large role in maintaining high thermal efficiencies during the heating mode during which turbulent flow conditions were in danger of not being met. Conversely, the ‘Smart Manifold’ proved relatively ineffective in months requiring cooling, offering little to no pump energy savings. This is because turbulence in cooling mode occurs at lower total system flow rates, making the ‘Smart Manifold’ unnecessary in much of the time in cooling mode.

The total energy savings for the ‘Smart Manifold’ case was calculated to be 7121.45 kWh per year, resulting in an annual reduction of 2143.56 kilograms of carbon dioxide. The significance of this value can be largely influenced by the price of electricity, as well as government incentives for reductions in energy or emissions. In Toronto, Ontario, Canada, the Ontario Power Authority offers $0.05 - $0.10 for every kWh saved [31]. So, the ‘Smart Manifold’ could qualify for incentives of $356.07 - $712.15. With the total estimate cost of the ‘Smart Manifold’ system being $4184.4 to $7258.80, the current incentives could play a role in further reducing payback periods, and making the investment more appealing.

Despite the promising results generated in this thesis, there still remains the potential for a great deal of future work. In particular, it would be highly valuable to quantify the level at which

laminar flow impedes heat transfer in comparison to turbulent flow. While industrial practice has a strong tendency to design systems for turbulence, it may be noteworthy to determine how vital turbulence truly is. The use of a computational fluid dynamic simulation would be one method by which this could be examined, or through a test borehole experiment in the field.

Another area for future study that may prove to be promising is the implementation of a 'Smart Manifold' in a building that is heating dominant. In the case study used in this thesis, the building was strongly cooling dominant. In a heating dominant building, the fluid temperature would remain low, which would correspond to a higher viscosity, and the need for higher flows to achieve turbulence. In Chapter 4, Case II, full pump capacity was needed in heating mode to achieve turbulence, but was only active for a short time. The short cycling of the pump indicates it is ineffectively used, and therefore longer cycles are favourable. A heating dominated building may provide a greater opportunity for a 'Smart Manifold' to generate electrical savings.

Finally, it would be advantageous to examine the effects of the 'Smart Manifold' with the energy models of a variety of buildings, in order to better understand the technology's full potential. Building size, occupancy, and a variety of other factors have an impact on the way a GSHP system performs, so it would also be advantageous to see the influence those factors have on the performance of the 'Smart Manifold' as well. By studying a wide variety of buildings and building types, it also allows for more statistical analysis.

Appendix A

In Appendix A, a summary of the energy model is given and the results of Section 4 are summarized. Table 7 is a summary of the hourly corrected cooling and heating demand. The corrected demand was described in Chapter 3, with the assumption that in a single hour only either heating or cooling can be provided by the GSHP system. Table 8 summarizes circulation pump run time and electricity consumption for each of the cases.

Table 7 – Building Energy Model Results, Courtesy of [38]

Hour	Corrected Cooling Demand (kBTU)	Corrected Heating Demand (kBTU)
1	0	397.41
2	0	458.06
3	0	506.42
4	0	505.13
5	0	445.22
…	…	…
4380	975.00	0
…	…	…
5756	0	51.96
8757	0	81.47
8758	0	128.27
8759	0	190.22
8760	0	286.42

Table 8 – Run Time and Power Consumption Results

	Case I		Case II		Case III	
Hour	Pump Run Time (minutes)	Power Consumption (kWh)	Pump Run Time (minutes)	Power Consumption (kWh)	Pump Run Time (minutes)	Power Consumption (kWh)
1	13.7	4.1	13.7	4.1	33.0	0.7
2	15.8	4.7	15.8	4.7	38.0	0.8
3	17.5	5.2	17.5	5.2	35.0	1.3
4	17.5	5.2	17.5	5.2	34.9	1.3
5	15.4	4.6	15.4	4.6	36.9	0.8
…	…	…	…	…	…	…
4380	20.4	6.1	40.6	1.5	40.6	1.5
…	…	…	…	…	…	…
5756	0	0	0	0	0	0
8757	0	0	0	0	0	0
8758	9.3	2.8	9.3	2.8	37.1	0.2
8759	6.6	2.0	6.6	2.0	39.4	0.1
8760	9.9	2.9	9.9	2.9	39.6	0.2

Appendix B

Appendix B includes properties for 30% Propylene Glycol.

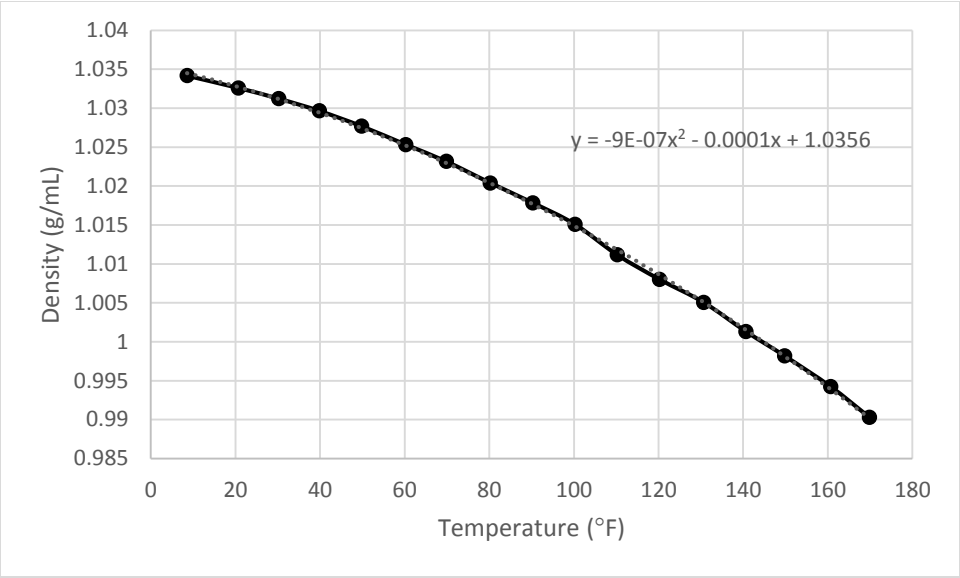

Figure 48 – Densities of 30% Propylene Glycol, reproduced from data from [44]

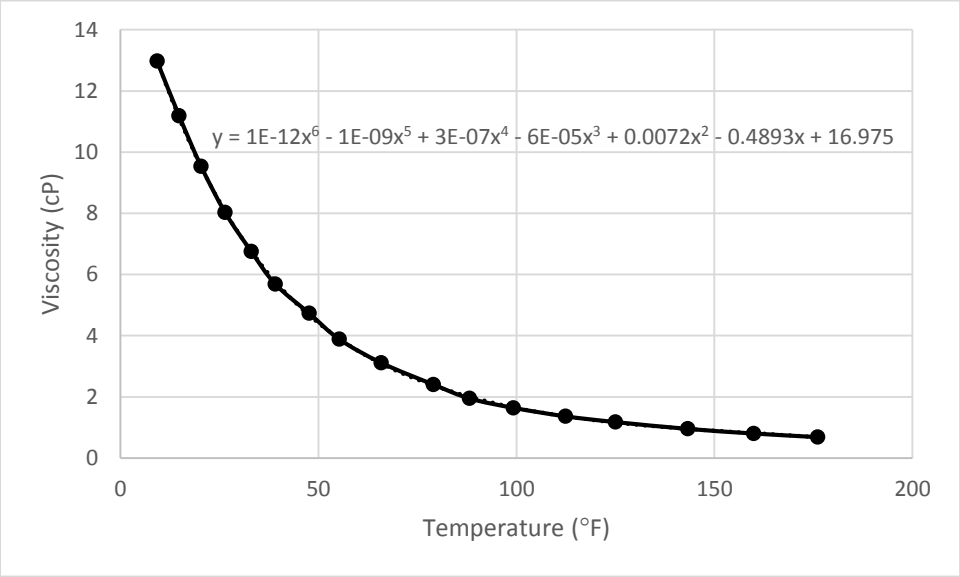

Figure 49 – Viscosity of 30% Propylene Glycol, reproduced from data from [44]

Specific Heat at 60°F: 0.935 $BTU/lb\ °F$ [44]

REFERENCES

[1] P. Blum, G. Campillo, W. Munch and K. Thomas, "CO2 Savings of Ground Source Heat Pump Systems - A Regional Analysis," *Renewable Energy*, pp. 122-127, 2009.

[2] M. Bonte, P. Stuyfzand, A. Hulsmann and P. Van Beelen, "Underground Thermal Energy Storage: Environmental Risks and Policy Development in the Netherlands and European Union," *Ecology and Society*, 2011.

[3] L. Rybach, "Geothermal Sustainability," GEOWATT AG, Zurich, 2007.

[4] G. Di Rezze, C. Negri and S. Esmail, *Personal Communication with Groundheat Solar Wind,* 2013.

[5] R. Xia and G. Di Rezze, "Thermal Response Test for Kelix GHE System," *Journal of Energy and Power Engineering*, pp. 1066-1072, 2013.

[6] R. Schellschmidt, B. Sanner, S. Pester and R. Schulz, "Geothermal Energy Use in Germany," in *World Geothermal Congress 2010*, Bali, 2010.

[7] F. De Ridder, M. Diehl, G. Mulder, J. Desmedt and J. Van Bael, "An Optimal Control Algorithm for Borehole Thermal Energy Storage Systems," *Energy and Buildings*, pp. 2918-2925, 2011.

[8] Natural Resources Canada, "saveonenergy," 2007. [Online]. Available: https://saveonenergy.ca/Consumer/Programs/New-Residential-Construction.aspx. [Accessed 2013].

[9] A. Benazza, E. Blanco, M. Aichouba, J. L. Rio and S. Laouedj, "Numerical Investigation of Horizontal Ground Coupled Heat Exchanger," *Energy Procedia*, pp. 29-35, 2011.

[10] V. Tarnawski, W. Leong and Y. Hamada, "Analysis of Ground Source Heat Pumps with Horizontal Ground Heat Exchangers for Northern Japan," *Renewable Energy*, pp. 127-134, 2009.

[11] K. S. Lee, "A Review on Concepts, Applications, and Models of Aquifer Thermal Energy Storage Systems," *Energies*, pp. 1320-1334, 2010.

[12] Daikin McQuay, "Geothermal Heat Pump Resource Center," 2002. [Online]. Available: http://www.mcquay.com/mcquaybiz/literature/lit_systems/AppGuide/AG_31-008_Geothermal_021607b.pdf. [Accessed 2013].

[13] W. Eugster and B. Sanner, "Technological Status of Shallow Geothermal Energy in Europe," in *Proceedings European Geothermal Congress 2007*, Unterhaching , 2007.

[14] Agreenability, "Agreenability - For Twisted Green Ideas," 2011. [Online]. Available: http://www.agreenability.com/. [Accessed 2013].

[15] L. Rybach and J. Eugster, "Sustainability Aspects of Geothermal Heat Pumps," in *Proceedings, Twenty-Seventh Workshop on Geothermal Reservoir Engineering*, Standford University, 2002.

[16] A. Fernandez, E. Mands, B. Sanner, M. Saur and L. Novelle, "Underground Diurnal and Seasonal Energy Storage for a Cooling and Heating System in a Retail Building in Jerez de la Frontera Spain," in *The 12th International Conference on Energy Storage*, 2012.

[17] M. Abbas and B. Sanner, "Feasibility Investigation for Underground Cold Storage in Giza, Egypt," Neuchatel/Bern, 1999.

[18] E. Kjellson, G. Hellstrom and B. Perers, "Optimization of Systems with the Combination of Ground-Source Heat Pump and Solar Collectors in Dwellings," *Energy*, pp. 1-7, 2009.

[19] H. Yang, P. Cui and Z. Fang, "Vertical-Borehole Ground-Coupled Heat Pumps: A Review of Models and Systems," *Applied Energy*, pp. 16-27, 2010.

[20] Sibbitt, Onne, McClenahan, Thornton, Brunger, Kokko and Wong, "The Drake Landing Solar Community Project," in *Canadian Sol. Build.Conf.*, Calgary, 2007.

[21] Ing and Kruse, "Earth Heat Pipes as Earth Probe for Geothermal Heat Pumps," in *FKW Research Centre for Refrigeration and Heat Pumps*, Hannover, 2008.

[22] Kruse and Russmann, "The Status of Development and Research on CO2 Earth Heat Pipes for Geothermal Heat Pumps," in *International High Performance Buildings Conference*, 2010.

[23] eQUEST, "The Quick Energy Simulation Tool," [Online]. Available: http://www.doe2.com/equest/.

[24] TRNSYS, "Building Energy Simulation Tool," [Online]. Available: http://www.trnsys.com.

[25] GLD, "Ground Loop Design," [Online]. Available: http://www.groundloopdesign.com.

[26] GHP Systems Inc, "Fundamentals of Commercial Geothermal Wellfield Design," South Dakota, 2010.

[27] *Effective Energy Modeling Strategies Webinar.* [Performance]. Groundloop Design, 2013.

[28] Desmedt, Hoes and Lemmens, "First realization of a large ground source heat pump system with vertical borehole heat exchangers for a belgian office building," in *Warmtepomp Symp.*, 2008.

[29] Dincer and Rosen, Thermal Energy Storage: Systems and Applications 2nd Edition, 2011.

[30] Midttomme, Skarphagen and Borgnes, "Design and Operation of Ground-Source Heat Pump Systems for Heating and Cooling of Non-Residential Buildings," in *International IEA Heat Pump Conference*, Zurich, 2008.

[31] Ontario Power Authority, "SaveOnEnergy," 2014. [Online]. Available: https://www.saveonenergy.ca/Business/Program-Overviews/New-Construction/How-to-Participate.aspx.

[32] F. Ascione, L. Bellia and F. Minichiello, "Earth-to-Air Heat Exchangers for Italian Climates," *Renewable Energy*, pp. 2177-2188, 2011.

[33] University of Delaware, "Parallel Pipeline Systems," [Online]. Available: http://udel.edu/~inamdar/EGTE215/Parallel_flow.pdf. [Accessed 2014].

[34] W. Janna, Design of Fluid Thermal Systems, Stamford: Cengage Learning, 2011.

[35] Eaton Corporation, "Automation.com," November 2012. [Online]. Available: http://www.automation.com/pdf_articles/eaton/IA04008002E_VFD.Pumping-energysavings.pdf. [Accessed 2014].

[36] CEATI - Centre for Energy Advancement through Technological Innovation, "CEATI International," 2009. [Online]. Available: http://www.ceati.com/freepublications/7025_guide_web.pdf. [Accessed 2014].

[37] Y. Cengel and A. Ghajar, Heat and Mass Transfer - Fundamentals & Applications - Fourth Edition, New York: McGraw-Hill, 2011.

[38] M. Ghahfarrokhy, *Personal Communication: Building Energy Model Results*, 2014.

[39] S. Dworkin, W. Leong, P. Walsh, H. Nguyen, M. Alavy, M. Ayala, R. Hossain and M. Schlitt, "Geo-Cities Initiative: Supporting the Development of Earth Energy Systems in Urban Applications," Ryerson University, Toronto, 2013.

[40] W. Alzahrani, "Experimental Study of the Performance of a Vertical and a Horizontal Ground Loops Coupled to a Ground Source Heat Pump System," MASc Thesis, Department of Mechanical and Industrial Engineering, Ryerson University, Toronto, 2013.

[41] Ontario Energy Board, "Historical Electricity Prices," April 2014. [Online]. Available: http://www.ontarioenergyboard.ca/oeb/Consumers/Electricity/Electricity%20Prices/Historical%20Electricity%20Prices.

[42] Canadian Press, "The Financial Post," 2013. [Online]. Available: http://business.financialpost.com/2013/12/02/ontario-electricity-rates-to-keep-rising-as-long-term-energy-plan-released/?__lsa=cdc6-1e44.

[43] T. Hamilton, "Geothermal heating-cooling: Canadians are hot and cold about it," The Toronto Star, 2012. [Online]. Available: http://www.thestar.com/business/2012/02/17/geothermal_heatingcooling_canadians_are_hot_and_cold_about_it.html.

[44] The Dow Chemical Company, "dow.com," 2003. [Online]. Available: http://msdssearch.dow.com/PublishedLiteratureDOWCOM/dh_0047/0901b803800479d9.pdf?filepath=propyleneglycol/pdfs/noreg/117-01682.pdf&fromPage=GetDoc.